

[9]aneN₃-based fluorescent receptors for metal ion sensing featuring urea and amide functional groups.

Alessandra Garau, Andrea Bencini, Alexander J. Blake, Claudia Caltagirone, Luca Conti, Francesco Isaia, Vito Lippolis, Riccardo Montis, Palma Mariani, Mariano Andrea Scorciapino.

Electronic Supporting Information (ESI)

INDEX

1. Synthesis of 1,4,7-tris-(N-ethyl-N'-phenyl-2yl)-1,4,7-triazacyclononane (L1)
 2. Synthesis of 1,4,7-tris-(N-ethyl-N'-quinolin-2yl)-1,4,7-triazacyclononane (L2)
 3. Synthesis of 1,4,7-tris-(N-8-quinolinylacetamide)-1,4,7-triazacyclononane (L3)
 4. Synthesis of [ZnL1(Ac)](Ac) (1)
 5. Synthesis of [CuL1(Cl)](Cl) (2)
 6. Synthesis of [CuL3](NO₃) (3)
- Table S1 The stability constants (K_a , M^{-1})^a of 1:1 complexes of L1 and L2 with a variety of anionic guests
- Fig. S1 ¹H-NMR of L¹ with TBAF in DMSO-*d*₆
- Fig. S2 ¹H-NMR of L¹ with TBAAcO in DMSO-*d*₆
- Fig. S3 ¹H-NMR of L¹ with TBABzO in DMSO-*d*₆
- Fig. S4 ¹H-NMR of L¹ with TBAH₂PO₄ in DMSO-*d*₆
- Fig. S5 ¹H-NMR of L¹ with TBACl in DMSO-*d*₆
- Fig. S6 ¹H-NMR of L² with TBAAcO in DMSO-*d*₆
- Fig. S7 ¹H-NMR of L² with TBABzO in DMSO-*d*₆
- Fig. S8 ¹H-NMR of L² with TBAH₂PO₄ in DMSO-*d*₆
- Fig. S9 ¹H-NMR of L² with TBACl in DMSO-*d*₆
- Fig. S10 Absorption spectra of L2 upon addition of increasing amounts of Cd²⁺
- Fig. S11 Absorption spectra of L2 in the presence of increasing amounts of Zn²⁺
- Fig. S12 Absorption spectra of L2 in the presence of increasing amounts of Pb²⁺
- Fig. S13 Absorption spectra of L2 in the presence of increasing amounts of Cu²⁺
- Fig. S14 Changes in the emission spectrum of L2 upon addition of increasing amounts of Cd²⁺
- Fig. S15 Changes in the emission spectrum of L2 upon addition of increasing amounts of Zn²⁺
- Fig. S16 Changes in the emission spectrum of L2 upon addition of increasing amounts of Pb²⁺
- Fig. S17 Changes in the emission spectrum of L2 upon addition of increasing amounts of Cu²⁺
- Fig. S18 Normalized fluorescent intensity versus molar ratio plot for ligand L2 upon addition of increasing amounts of Cd²⁺, Zn²⁺, Pb²⁺ and Cu²⁺ ions
- Fig. S19 Distribution diagram of the protonated species of L3
- Fig. S20 Distribution diagrams of the species formed by Hg²⁺ with L3
- Fig. S21 Distribution diagrams of the species formed by Cu²⁺ with L3
- Fig. S22 Distribution diagrams of the species formed by Cd²⁺ with L3
- Fig. S23 Distribution diagrams of the species formed by Cd²⁺ with L3
- Fig. S24 Superimposition of the fluorescence emission intensity at 505 nm with the distribution diagrams of the species formed by L3 in the presence of Zn²⁺
- Fig. S25 High and low frequency region of the ¹H-NMR spectra of L3 in the presence of different amounts of Zn²⁺
- Fig. S26 Conformers for L3 in the absence of any metal ion.
- Fig. S27 Conformers for L3 in the presence of Zn²⁺
- Fig. S28 ESI-MS spectrum of a solution of L3 and Zn²⁺ at molar ratio Zn²⁺/L3 of 1.0
- Fig. S29 Low and high frequency regions of the ¹H-NMR spectra of L3 at different pH values
- Fig. S30 Low field and high field region of the ¹H-NMR spectra of L3 in the presence of different amounts of Hg²⁺
- Fig. S31 ESI-MS spectrum at molar ratio Hg²⁺/L3 of 1.0
- Fig. S32 ¹H-NMR spectra of a) solution of L3 and Zn²⁺ at molar ratio Zn²⁺/L3 of 0.5, b) solution of L3 and Zn²⁺ in 1:1 molar ratio and addition of 1 equiv. of Hg²⁺ and c) solution of L3 and Hg²⁺ at molar ratio Hg²⁺/L3 of 0.7.
- Fig. S33 ESI-MS spectrum of a solution of L3 and Zn²⁺ in 1:1 molar ratio and addition of 1 equiv. of Hg²⁺
- Table S2 Summary of the basic crystallographic parameters for [ZnL1(Ac)](Ac) (1), [CuL1(Cl)](Cl)·H₂O (2) and [CuL3](NO₃) (3)
- Table S3 Selected Bond Distances (Å) and Angles (°) for [ZnL1(Ac)](Ac) (1), [CuL1(Cl)](Cl)·H₂O (2) and [CuL3](NO₃) (3)

1. Synthesis of 1,4,7-tris-(N-ethyl-N'-phenyl-2yl)-1,4,7-triazacyclononane (L1).

To a solution of 1,4,7-tris(2-aminoethyl)-1,4,7-triazacyclononane (0.30 g, 1.16 mmol) in 70 mL of dry CH_2Cl_2 was added in 24 hours under reflux, phenyl-isocyanate (0.27 g, 3.5 mmol) in dry CH_2Cl_2 (30 mL). The white solid was taken off, and the solvent was removed under reduced pressure. The residue was dissolved in CH_2Cl_2 and washed with water. The organic phase was dried over Na_2SO_4 , and the solvent removed under reduced pressure to obtain a colourless oil (0.45 g, 63% yield). $^1\text{H-NMR}$ ($\text{DMSO-}d_6$, 400 MHz): δ_{H} 2.70-2.95 (m, 18H, $\text{CH}_2\text{CH}_2\text{NCH}_2$, $\text{NCH}_2\text{CH}_2\text{N}$), 3.14 (m, 6H, $\text{CH}_2\text{CH}_2\text{NH}$), 6.39 (s, 3H, NH), 6.92 (t, 3H, $J = 8.0$ Hz), 7.22 (t, 6H, $J = 8.0$ Hz), 7.36 (d, 6H, $J = 8.0$ Hz), 8.74 (s, 3H, NH). MS (ESI): m/z 615 ($[\text{C}_{33}\text{H}_{45}\text{N}_9\text{O}_3]^+$).

2. Synthesis of 1,4,7-tris-(N-ethyl-N'-quinolin-2yl)-1,4,7-triazacyclononane (L2).

To a solution of 1,4,7-tris(2-aminoethyl)-1,4,7-triazacyclononane (0.38 g, 1.47 mmol, 10 mL dry DMF) was added slowly quinolin-2-isocyanate (0.76 g, 4.41 mmol) in dry DMF (15 mL). The reaction mixture was stirred at room temperature for 48 hours under nitrogen, and the solvent was removed under reduced pressure. The residue was dissolved in CH_2Cl_2 and washed with water. The organic phase was dried over Na_2SO_4 , and the solvent removed under reduced pressure. The solid was crystallized with methanol to give a white solid (0.25 g, 22% yield). Anal. Found (Calcd) for $\text{C}_{42}\text{H}_{48}\text{N}_{12}\text{O}_3$: C, 66.0 (65.6); H, 6.5 (6.3); N, 21.5 (21.9%). $^1\text{H-NMR}$ ($\text{DMSO-}d_6$, 400 MHz): δ_{H} 2.58-2.72 (m, 18H, $\text{CH}_2\text{CH}_2\text{NCH}_2$, $\text{NCH}_2\text{CH}_2\text{N}$), 3.20-3.25 (m, 6H, $\text{CH}_2\text{CH}_2\text{NH}$), 7.31 (d, 6H, $J = 8.0$ Hz), 7.34 (t, 3H, $J = 8.0$ Hz), 7.75 (t, 3H, $J = 8.0$ Hz), 8.15 (d, 6H, $J = 8.0$ Hz), 8.70 (s, 3H, NH), 9.48 (s, 3H, NH). MS (ESI): m/z 768 ($[\text{C}_{42}\text{H}_{48}\text{N}_{12}\text{O}_3]^+$).

3. Synthesis of 1,4,7-tris-(N-8-quinolinylacetamide)-1,4,7-triazacyclononane (L3).

To a solution of 1,4,7-triazacyclononane (0.10 g, 0.77 mmol) and K_2CO_3 (0.64 g, 4.6 mmol) was added 2-chloro-N-8-quinolinylacetamide (0.53 g, 2.4 mmol) in anhydrous acetonitrile (30 mL). The reaction mixture was heated at 80°C for 24 hours under nitrogen. The solid was filtered off, and the solvent was removed under reduced pressure. The residue was dissolved in CH_2Cl_2 and washed with water. The organic phase was dried over Na_2SO_4 , and the solvent removed under reduced pressure. The solid was washed overnight with Et_2O to give pale yellow solid (0.25 g, 47% yield). Anal. Found (Calcd) for $\text{C}_{39}\text{H}_{39}\text{N}_9\text{O}_3$: C, 68.3 (68.7); H, 5.6 (5.8); N, 18.2 (18.5%). $^1\text{H-NMR}$ (CDCl_3 , 500 MHz): δ_{H} 3.39 (s, 12H, $\text{NCH}_2\text{CH}_2\text{N}$), 3.51 (s, 6H, NCH_2CO), 7.43 (dd, $J = 8.3, 4.1$ Hz, 3H), 7.54 (m, 6H), 8.20 (dd, $J = 6.8, 1.5$ Hz, 3H), 8.71 (dd, $J = 2.65, 1.5$ Hz, 3H), 8.74 (dd, $J = 4.9, 1.95$ Hz, 3H), 11.19 (s, 3H, NH). $^{13}\text{C-NMR}$ (CDCl_3 , 100 MHz): δ_{C} 57.18 ($\text{NCH}_2\text{CH}_2\text{N}$), 64.90 (NCH_2CO), 116.53, 122.34, 122.50, 127.65, 128.77, 135.09, 136.95, 139.08, 149.23 (aromatic carbon), 170.36 (CO). ESI-MS: m/z 682 ($[\text{C}_{39}\text{H}_{39}\text{N}_9\text{O}_3]^+$).

4. Synthesis of $[\text{ZnL1}(\text{Ac})](\text{Ac})$ (1). $\text{Zn}(\text{Ac})_2$ (3.0 mg, 0.016 mmol) in MeCN (1 mL) was added to a solution of L1 (10.0 mg, 0.016 mmol) in MeCN (5 mL). The solution was stirred at room temperature for 2 hours and colourless crystals were obtained by diffusion of Et_2O vapour in the solution (60% yield). Anal. Found (Calcd) for $\text{C}_{37}\text{H}_{51}\text{N}_9\text{O}_7\text{Zn}$: C, 55.2 (55.6); H, 6.2 (6.4); N, 15.4 (15.8%).

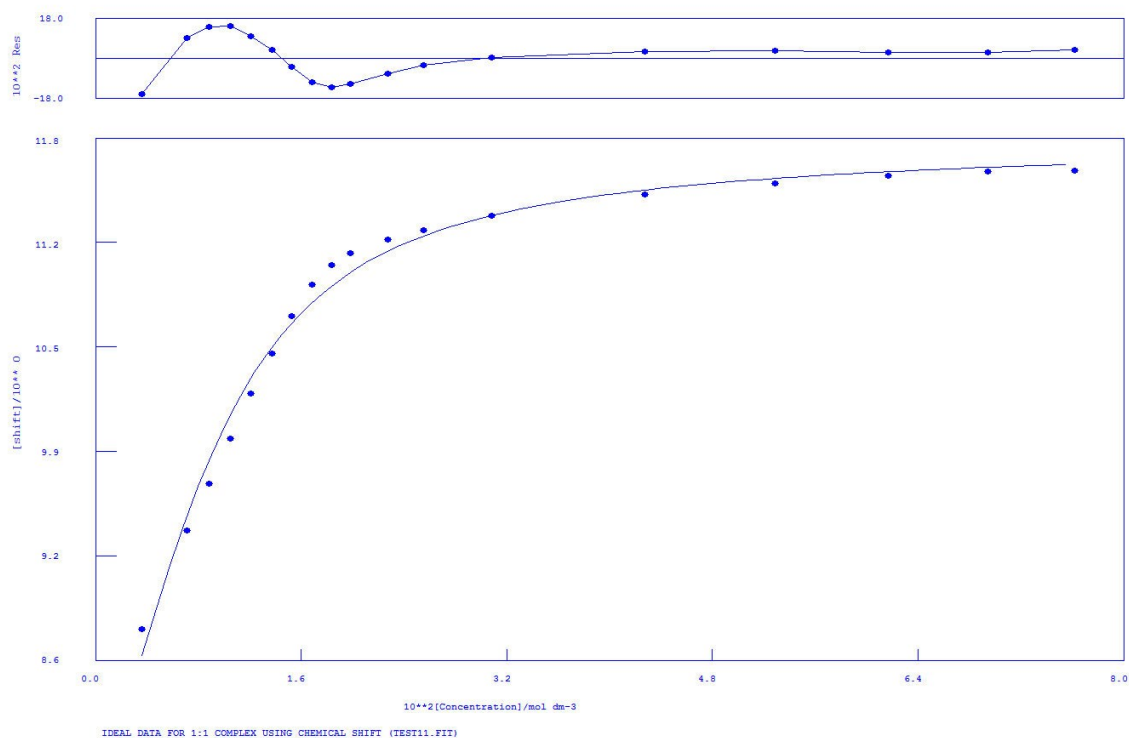
5. Synthesis of $[\text{CuL1}(\text{Cl})](\text{Cl})$ (2). CuCl_2 (2.0 mg, 0.016 mmol) in MeCN (1 mL) was added to a solution of L1 (10.0 mg, 0.016 mmol) in MeCN (5 mL). The solution was stirred at room temperature for 2 hours and blue crystals were obtained by diffusion of Et_2O vapour in the solution (65% yield). Anal. Found (Calcd) for $\text{C}_{33}\text{H}_{46}\text{Cl}_2\text{CuN}_9\text{O}_{3.5}$: C, 51.8 (52.2); H, 6.2 (6.1); N, 16.2 (16.6%).

6. Synthesis of $[\text{CuL3}](\text{NO}_3)$ (3). $\text{Zn}(\text{NO}_3)_2 \cdot 6\text{H}_2\text{O}$ (4.0 mg, 0.015 mmol) in MeCN (1 mL) was added to a solution of L3 (10.0 mg, 0.015 mmol) in MeCN (5 mL). The solution was stirred at room temperature for 2 hours and light blue crystals were obtained by diffusion of Et_2O vapour in the solution (68% yield). Anal. Found (Calcd) for $\text{C}_{39}\text{H}_{38}\text{CuN}_{10}\text{O}_6$: C, 57.8 (58.1); H, 4.5 (4.7); N, 17.1 (17.4%).

Table S1. The stability constants (K_a , M^{-1})^a of 1:1 complexes of L1 and L2 with a variety of anionic guests (added as TBA salts) at 298K in DMSO-*d*₆ as determined by following the NH resonance of the urea unit.

Anion	L1	L2
H ₂ PO ₄ ⁻	173	32
F ⁻	366	deprot.
Cl ⁻	17	<10
AcO ⁻	67	<10
BzO ⁻	42	16

^a Errors on association constants are ≤13% (L2 with H₂PO₄⁻ and AcO⁻ 20% and 28%, respectively).



Calculations by WinEQNMR Version 1.20 by Michael J. Hynes
Program run at 11:10:27 on 05/07/2012

IDEAL DATA FOR 1:1 COMPLEX USING CHEMICAL SHIFT (TEST11.FIT)

Reaction: M + L = ML

FILE: TEST11.FIT

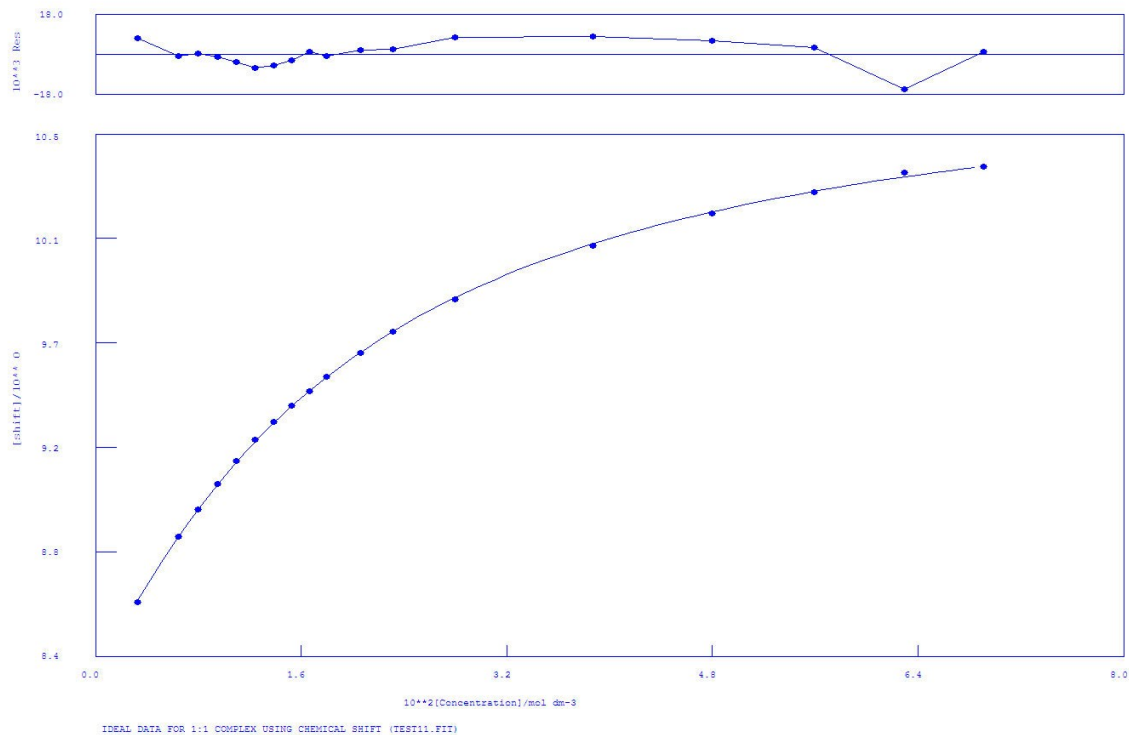
IDEAL DATA: K1 = 63.091; DELTA M = 20.0; DELTA ML = 120.0

File prepared by M. J. Hynes, October 22 2000

NO. A PARAMETER DELTA ERROR CONDITION DESCRIPTION

1 1 3.65559E+02 2.000E-01 4.897E+01 8.457E+00 K1
2 1 7.54357E+00 2.000E-01 1.343E-01 3.312E+00 SHIFT M
3 1 1.18062E+01 1.000E+00 6.314E-02 4.603E+00 SHIFT ML

Figure S1. ¹H-NMR of L¹ with TBAF in DMSO-*d*₆. The fitting has been obtained following the most downfield shifted NH proton.



Calculations by WinEQNMR Version 1.20 by Michael J. Hynes
 Program run at 09:06:19 on 03/11/2010

IDEAL DATA FOR 1:1 COMPLEX USING CHEMICAL SHIFT (TEST11.FIT)

Reaction: $M + L = ML$

FILE: TEST11.FIT

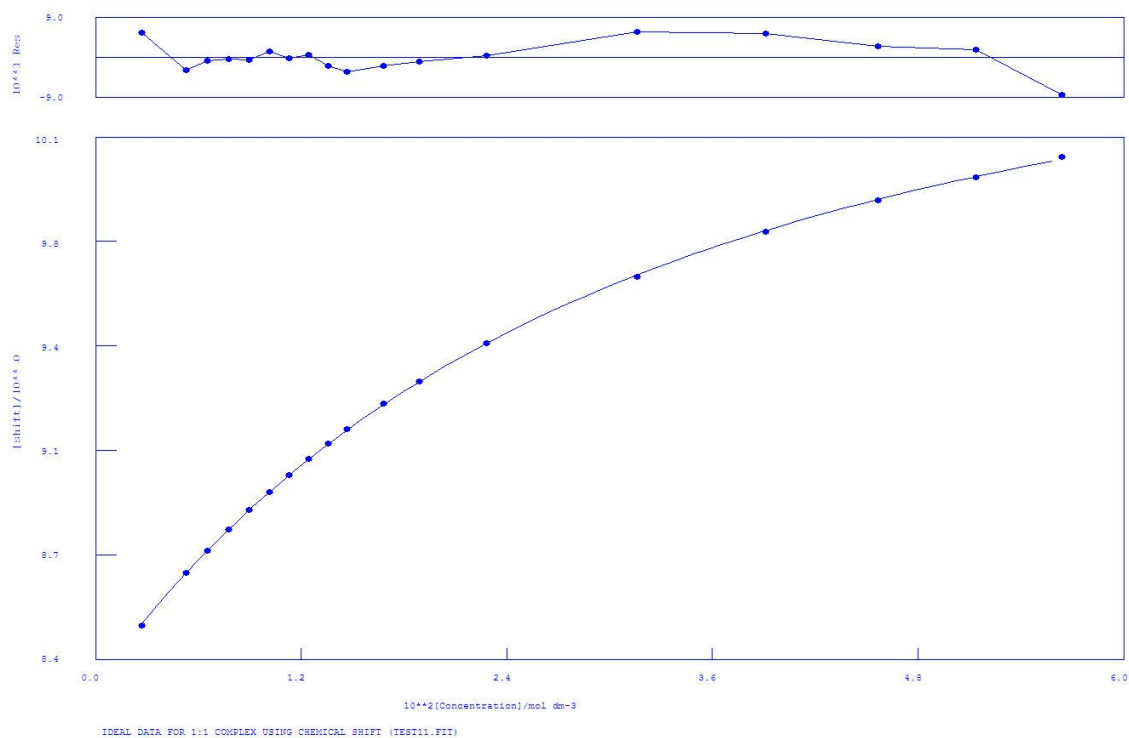
IDEAL DATA: $K_1 = 63.091$; $\Delta M = 20.0$; $\Delta ML = 120.0$

File prepared by M. J. Hynes, October 22 2000

NO. A PARAMETER DELTA ERROR CONDITION DESCRIPTION

1	1	6.67075E+01	2.000E-01	1.142E+00	3.082E+01	K1
2	1	8.30769E+00	2.000E-01	7.169E-03	7.386E+00	SHIFT M
3	1	1.08720E+01	1.000E+00	1.052E-02	1.480E+01	SHIFT ML

Figure S2. $^1\text{H-NMR}$ of L^1 with TBAAcO in $\text{DMSO-}d_6$. The fitting has been obtained following the most downfield shifted NH proton.



Calculations by WinEQNMR Version 1.20 by Michael J. Hynes
 Program run at 10:35:12 on 03/11/2010

IDEAL DATA FOR 1:1 COMPLEX USING CHEMICAL SHIFT (TEST11.FIT)

Reaction: $M + L = ML$

FILE: TEST11.FIT

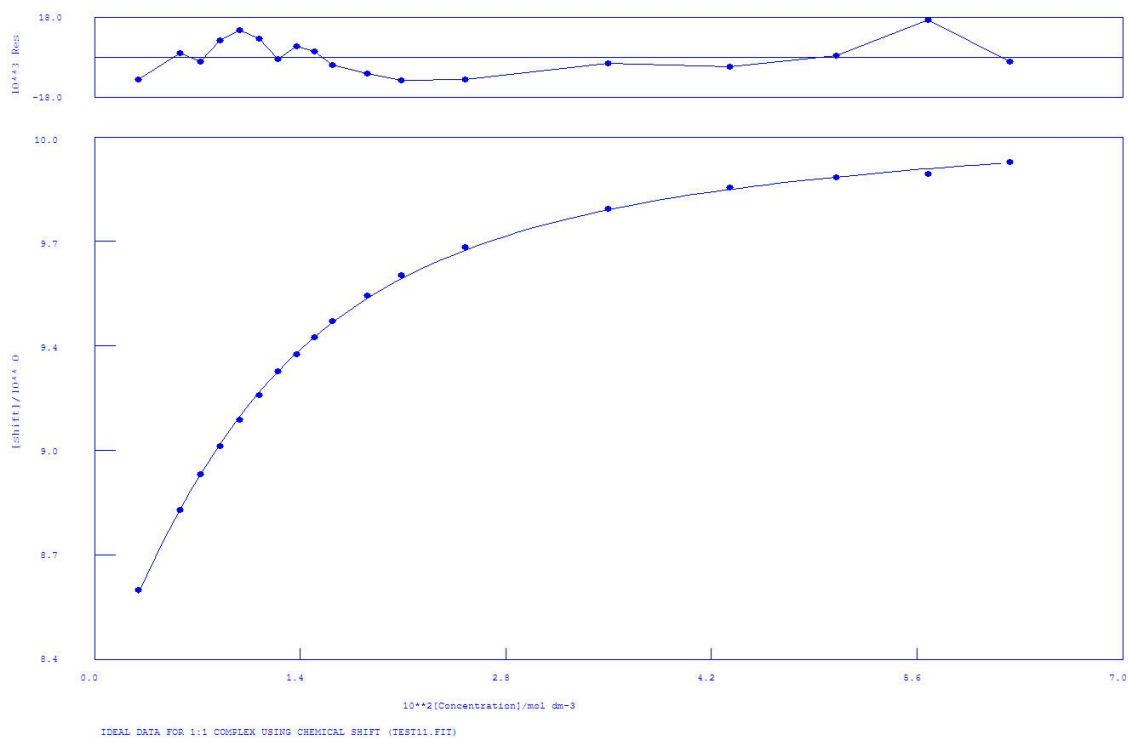
IDEAL DATA: $K_1 = 63.091$; $\Delta M = 20.0$; $\Delta ML = 120.0$

File prepared by M. J. Hynes, October 22 2000

NO. A PARAMETER DELTA ERROR CONDITION DESCRIPTION

1	1	4.21288E+01	2.000E-01	6.213E-01	5.856E+01	K1
2	1	8.32517E+00	2.000E-01	3.636E-03	7.757E+00	SHIFT M
3	1	1.08375E+01	1.000E+00	1.260E-02	3.444E+01	SHIFT ML

Figure S3. $^1\text{H-NMR}$ of L^1 with TBABzO in $\text{DMSO-}d_6$. The fitting has been obtained following the most downfield shifted NH proton.



Calculations by WinEQNMR Version 1.20 by Michael J. Hynes
 Program run at 10:09:42 on 03/11/2010

IDEAL DATA FOR 1:1 COMPLEX USING CHEMICAL SHIFT (TEST11.FIT)

Reaction: $M + L = ML$

FILE: TEST11.FIT

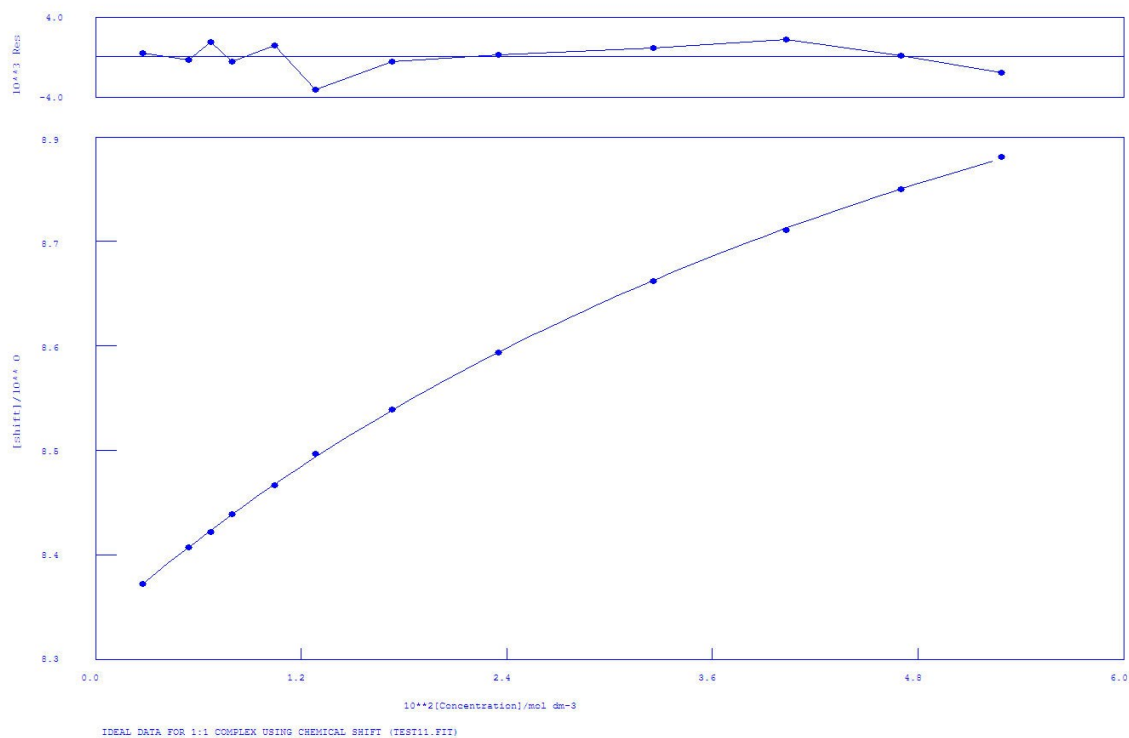
IDEAL DATA: $K_1 = 63.091$; $\Delta M = 20.0$; $\Delta ML = 120.0$

File prepared by M. J. Hynes, October 22 2000

NO. A PARAMETER DELTA ERROR CONDITION DESCRIPTION

1	1	1.72872E+02	2.000E-01	4.654E+00	1.522E+01	K1
2	1	8.28291E+00	2.000E-01	9.750E-03	4.813E+00	SHIFT M
3	1	1.00970E+01	1.000E+00	8.105E-03	7.562E+00	SHIFT ML

Figure S4. $^1\text{H-NMR}$ of L^1 with TBAH_2PO_4 in $\text{DMSO-}d_6$. The fitting has been obtained following the most downfield shifted NH proton.



Calculations by WinEQNMR Version 1.20 by Michael J. Hynes
 Program run at 09:50:07 on 03/15/2010

IDEAL DATA FOR 1:1 COMPLEX USING CHEMICAL SHIFT (TEST11.FIT)

Reaction: $M + L = ML$

FILE: TEST11.FIT

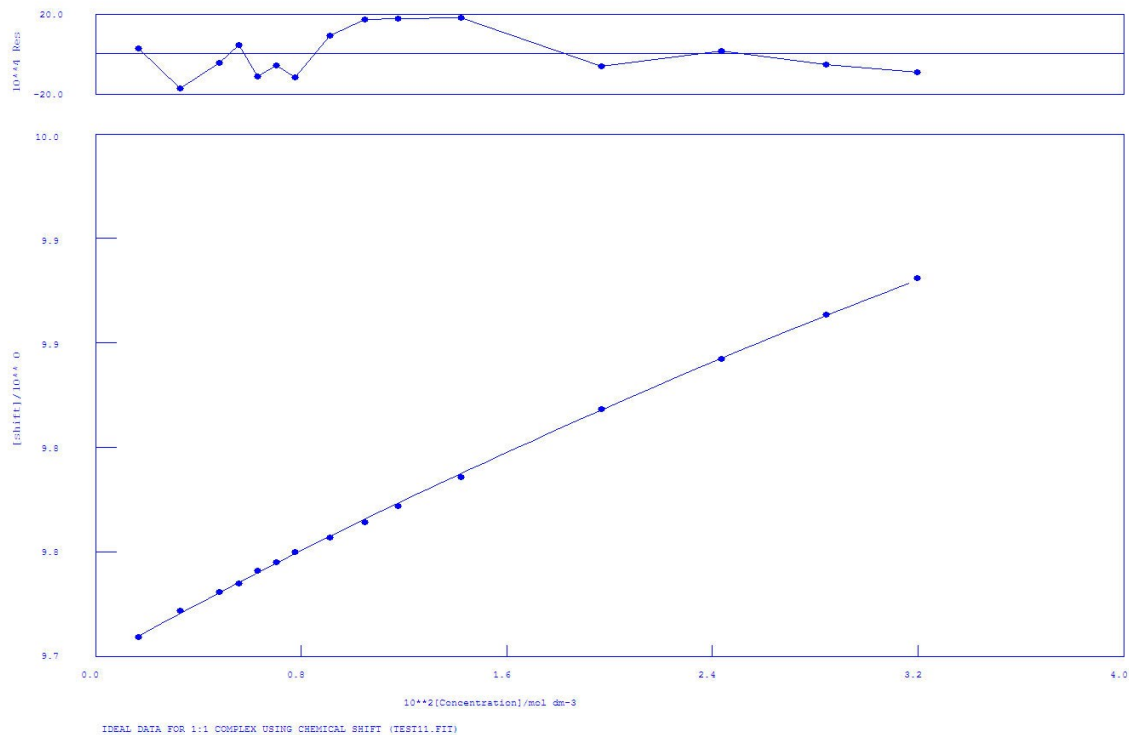
IDEAL DATA: $K_1 = 63.091$; $\Delta M = 20.0$; $\Delta ML = 120.0$

File prepared by M. J. Hynes, October 22 2000

NO. A PARAMETER DELTA ERROR CONDITION DESCRIPTION

1	1.73529E+01	2.000E-01	6.043E-01	1.738E+02	K1
2	8.33678E+00	2.000E-01	1.453E-03	6.549E+00	SHIFT M
3	9.40885E+00	1.000E+00	1.951E-02	1.351E+02	SHIFT ML

Figure S5. $^1\text{H-NMR}$ of L^1 with TBACl in $\text{DMSO-}d_6$. The fitting has been obtained following the most downfield shifted NH proton.



Calculations by WinEQNMR Version 1.20 by Michael J. Hynes
 Program run at 09:26:23 on 07/09/2012

IDEAL DATA FOR 1:1 COMPLEX USING CHEMICAL SHIFT (TEST11.FIT)

Reaction: $M + L = ML$

FILE: TEST11.FIT

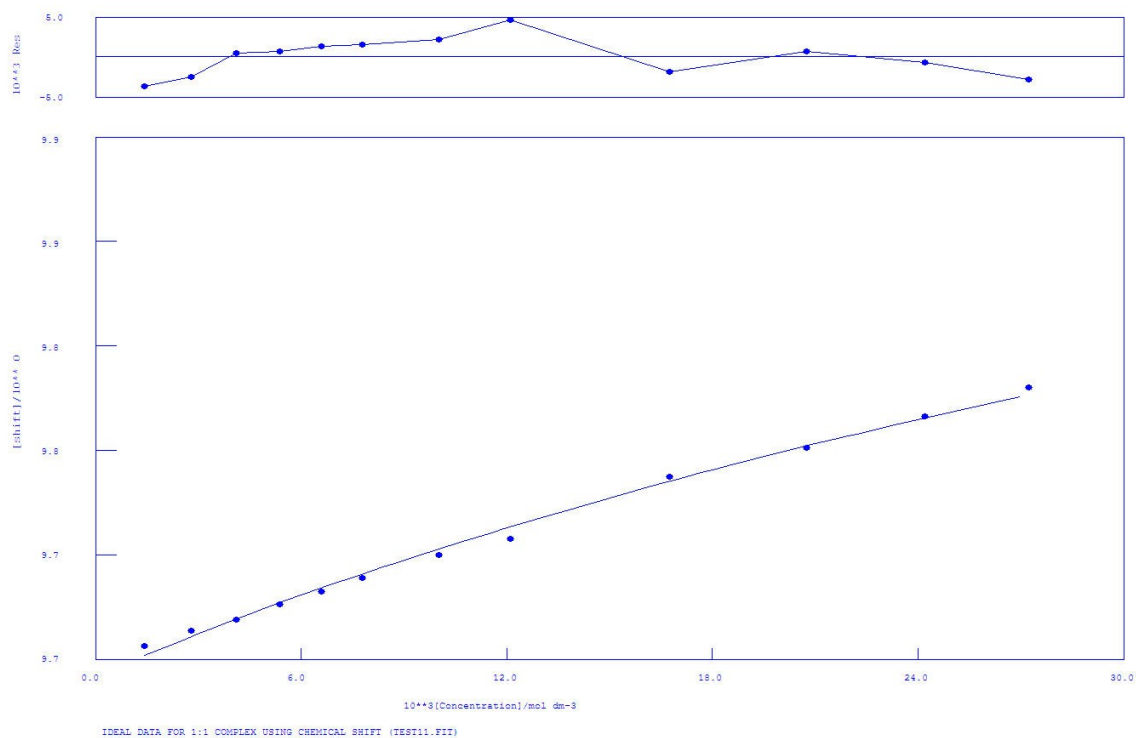
IDEAL DATA: $K_1 = 63.091$; $\Delta M = 20.0$; $\Delta ML = 120.0$

File prepared by M. J. Hynes, October 22 2000

NO. A PARAMETER DELTA ERROR CONDITION DESCRIPTION

1	1	6.60500E+00	2.000E-01	7.796E-01	1.192E+03	K1
2	1	9.69753E+00	2.000E-01	1.028E-03	9.114E+00	SHIFT M
3	1	1.09741E+01	1.000E+00	1.198E-01	1.057E+03	SHIFT ML

Figure S6. $^1\text{H-NMR}$ of L^2 with TBAAcO in $\text{DMSO-}d_6$. The fitting has been obtained following the most downfield shifted NH proton.



Calculations by WinEQNMR Version 1.20 by Michael J. Hynes
 Program run at 09:33:01 on 07/09/2012

IDEAL DATA FOR 1:1 COMPLEX USING CHEMICAL SHIFT (TEST11.FIT)

Reaction: $M + L = ML$

FILE: TEST11.FIT

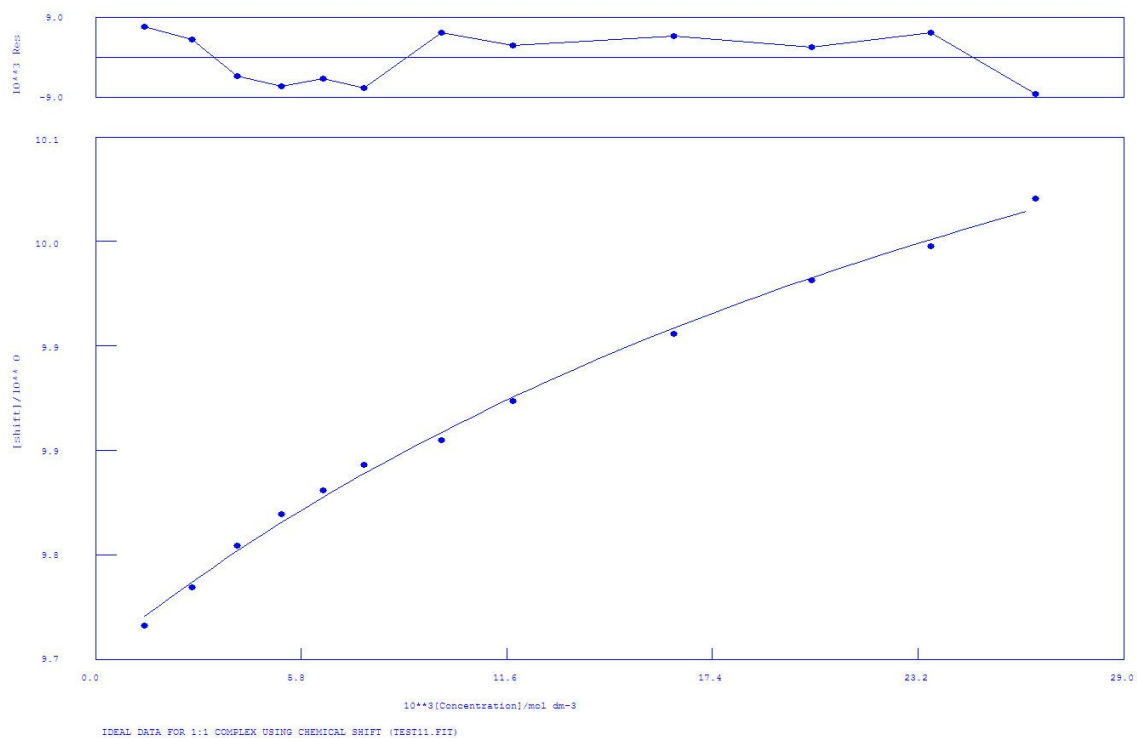
IDEAL DATA: $K_1 = 63.091$; $\Delta M = 20.0$; $\Delta ML = 120.0$

File prepared by M. J. Hynes, October 22 2000

NO. A PARAMETER DELTA ERROR CONDITION DESCRIPTION

1	1	1.63545E+01	2.000E-01	4.516E+00	2.587E+02	K1
2	1	9.69360E+00	2.000E-01	1.932E-03	4.837E+00	SHIFT M
3	1	1.00531E+01	1.000E+00	6.779E-02	2.233E+02	SHIFT ML

Figure S7. $^1\text{H-NMR}$ of L^2 with TBABzO in $\text{DMSO-}d_6$. The fitting has been obtained following the most downfield shifted NH proton.



Calculations by WinEQNMR Version 1.20 by Michael J. Hynes
 Program run at 09:39:45 on 07/09/2012

IDEAL DATA FOR 1:1 COMPLEX USING CHEMICAL SHIFT (TEST11.FIT)

Reaction: $M + L = ML$

FILE: TEST11.FIT

IDEAL DATA: $K_1 = 63.091$; $\Delta M = 20.0$; $\Delta ML = 120.0$

File prepared by M. J. Hynes, October 22 2000

NO. A PARAMETER DELTA ERROR CONDITION DESCRIPTION

1	1	3.21314E+01	2.000E-01	6.465E+00	1.915E+02	K1
2	1	9.70390E+00	2.000E-01	6.141E-03	7.097E+00	SHIFT M
3	1	1.04780E+01	1.000E+00	8.593E-02	1.483E+02	SHIFT ML

Figure S8. $^1\text{H-NMR}$ of L^2 with TBAH_2PO_4 in $\text{DMSO-}d_6$. The fitting has been obtained following the most downfield shifted NH proton.



Calculations by WinEQNMR Version 1.20 by Michael J. Hynes
Program run at 09:52:48 on 07/09/2012

IDEAL DATA FOR 1:1 COMPLEX USING CHEMICAL SHIFT (TEST11.FIT)

Reaction: M + L = ML

FILE: TEST11.FIT

IDEAL DATA: K1 = 63.091; DELTA M = 20.0; DELTA ML = 120.0

File prepared by M. J. Hynes, October 22 2000

NO. A PARAMETER DELTA ERROR CONDITION DESCRIPTION

1	1	4.60500E+00	2.000E-01	2.796E-01	1.192E+03	K1
2	1	9.69753E+00	2.000E-01	1.028E-03	9.114E+00	SHIFT M
3	1	1.09741E+01	1.000E+00	1.198E-01	1.057E+03	SHIFT ML

Figure S9. ^1H -NMR of L^2 with TBACl in $\text{DMSO}-d_6$. The fitting has been obtained following the most downfield shifted NH proton.

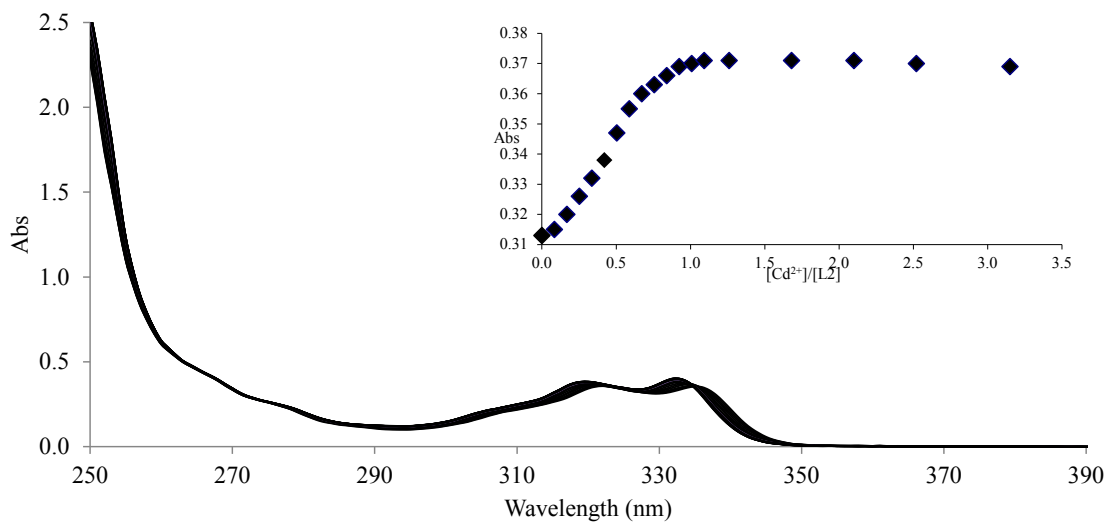


Figure S10. Absorption spectra of L2 upon addition of increasing amounts of Cd²⁺ (inset: absorbance values measured at 335 nm versus [Cd²⁺]/[L2] molar ratio, [L2] = 1.99·10⁻⁵ M, 25°C).

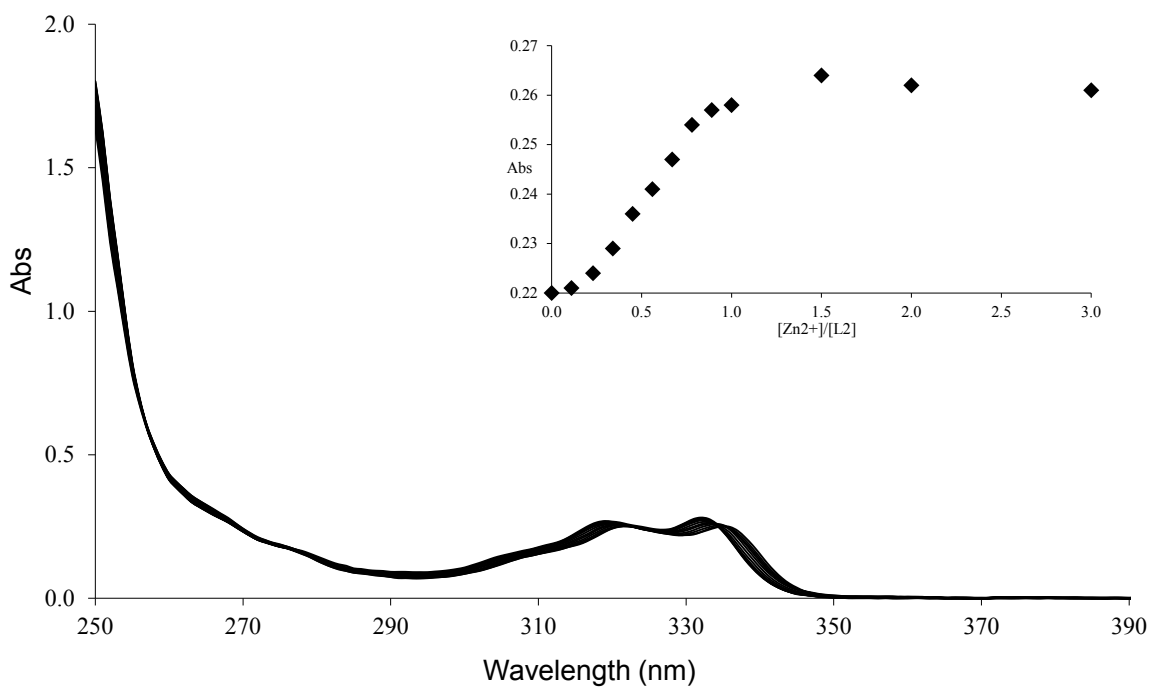


Figure S11. Absorption spectra of L2 in the presence of increasing amounts of Zn²⁺ (inset: absorbance values measured at 335 nm versus [Zn²⁺]/[L2] molar ratio, [L2] = 1.99·10⁻⁵ M, 25°C).

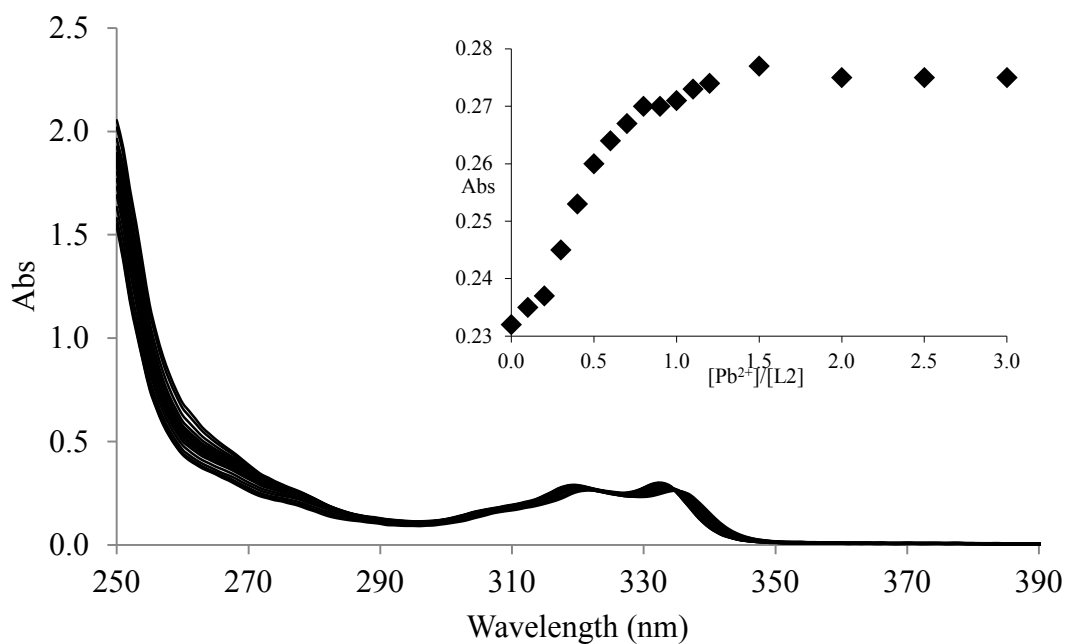


Figure S12. Absorption spectra of L2 in the presence of increasing amounts of Pb²⁺ (inset: absorbance values measured at 335 nm versus [Pb²⁺]/[L2] molar ratio, [L2] = 1.99·10⁻⁵ M, 25°C).

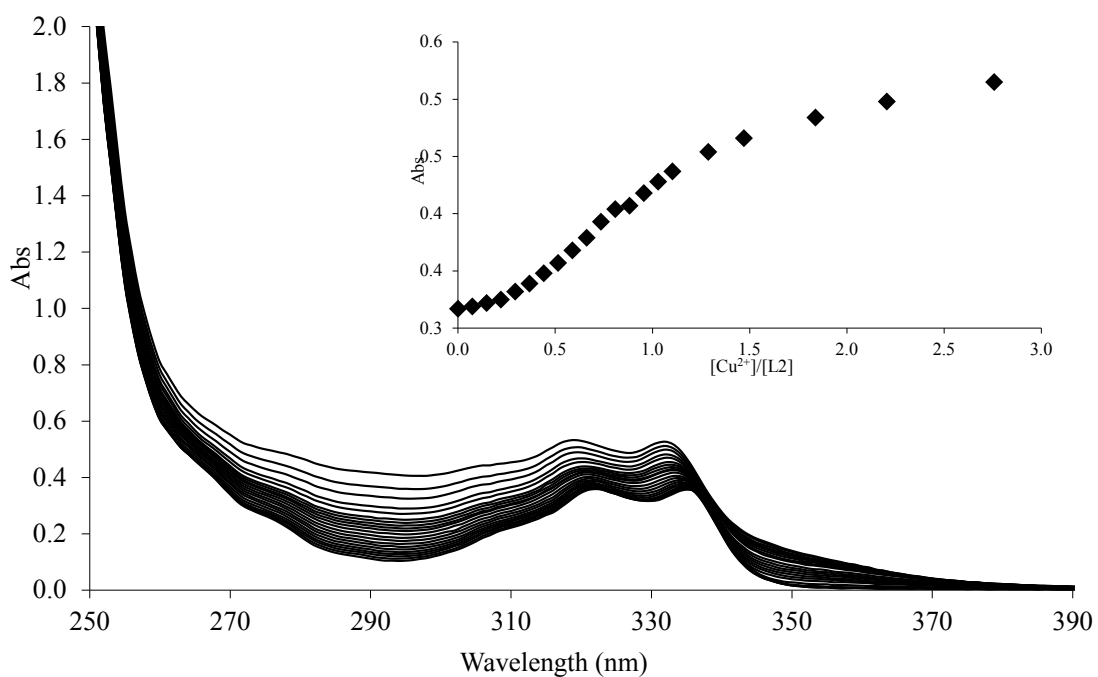


Figure S13. Absorption spectra of L2 in the presence of increasing amounts of Cu²⁺ (inset: absorbance values measured at 335 nm versus [Cu²⁺]/[L2] molar ratio, [L2] = 1.99·10⁻⁵ M, 25°C).

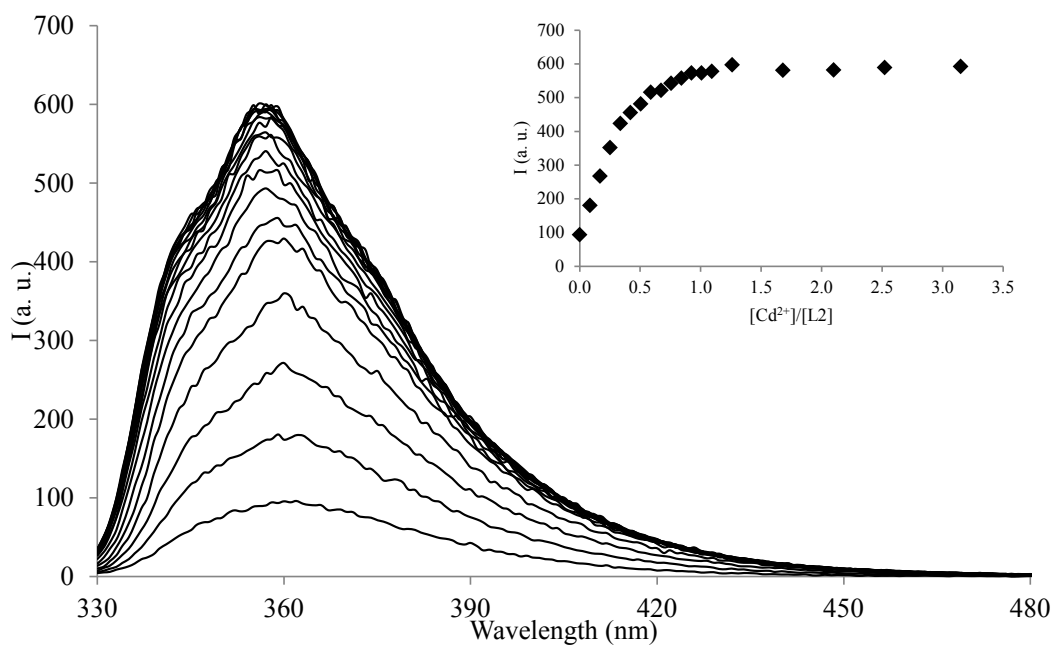


Figure S14. Changes in the emission spectrum of L2 upon addition of increasing amounts of Cd^{2+} (inset: emission values measured at 358 nm versus $[\text{Cd}^{2+}]/[\text{L2}]$ molar ratio, $[\text{L2}] = 1.99 \cdot 10^{-5} \text{ M}$, 25°C , $\lambda_{\text{ex}} = 323 \text{ nm}$).

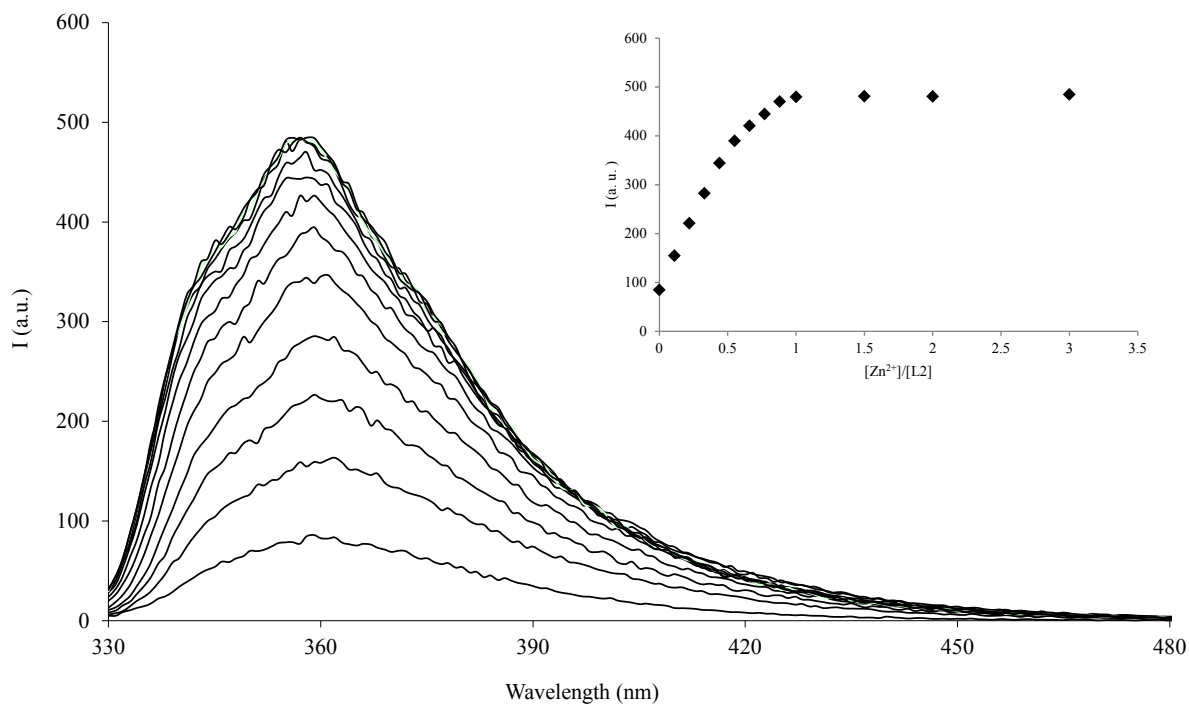


Figure S15. Changes in the emission spectrum of L2 upon addition of increasing amounts of Zn^{2+} (inset: emission values measured at 358 nm versus $[\text{Zn}^{2+}]/[\text{L2}]$ molar ratio, $[\text{L2}] = 1.99 \cdot 10^{-5} \text{ M}$, 25°C , $\lambda_{\text{ex}} = 323 \text{ nm}$).

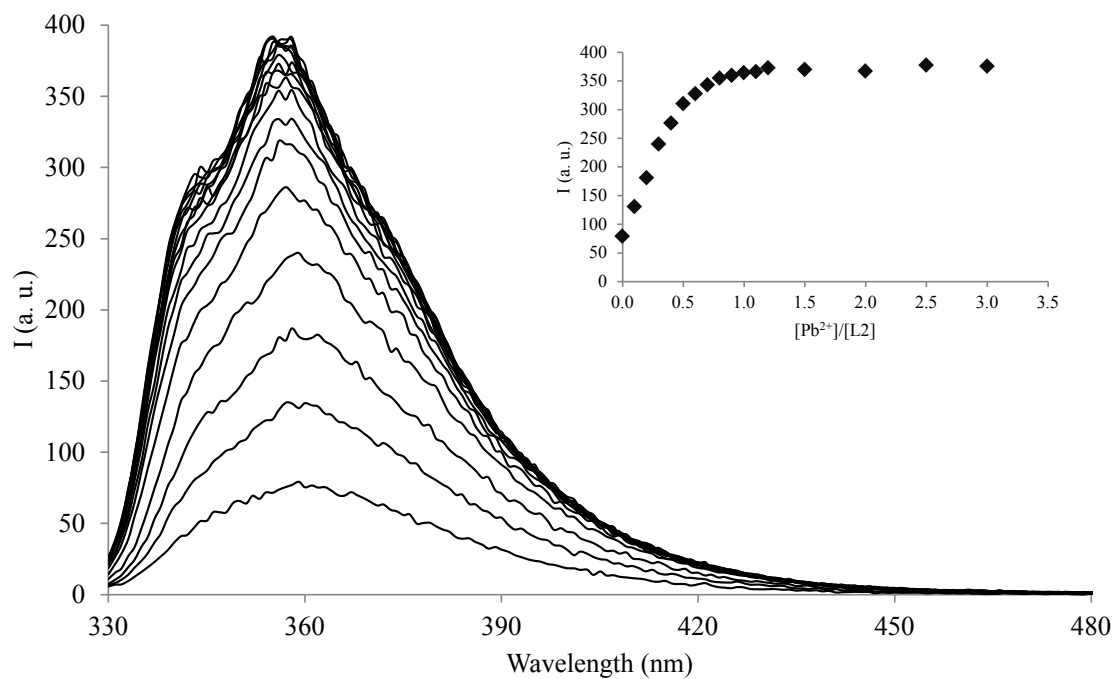


Figure S16. Changes in the emission spectrum of L2 upon addition of increasing amounts of Pb^{2+} (inset: emission values measured at 358 nm versus $[\text{Pb}^{2+}]/[\text{L2}]$ molar ratio, $[\text{L2}] = 1.99 \cdot 10^{-5} \text{ M}$, 25°C , $\lambda_{\text{ex}} = 323 \text{ nm}$).

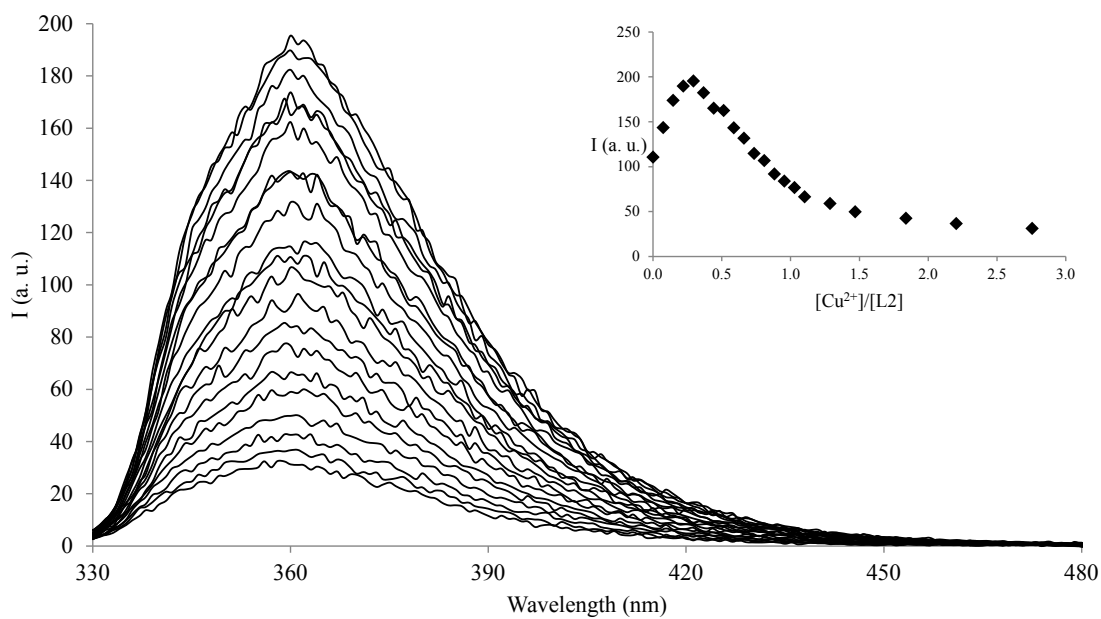


Figure S17. Changes in the emission spectrum of L2 upon addition of increasing amounts of Cu^{2+} (inset: emission values measured at 358 nm versus $[\text{Cu}^{2+}]/[\text{L2}]$ molar ratio, $[\text{L2}] = 1.99 \cdot 10^{-5} \text{ M}$, 25°C , $\lambda_{\text{ex}} = 323 \text{ nm}$).

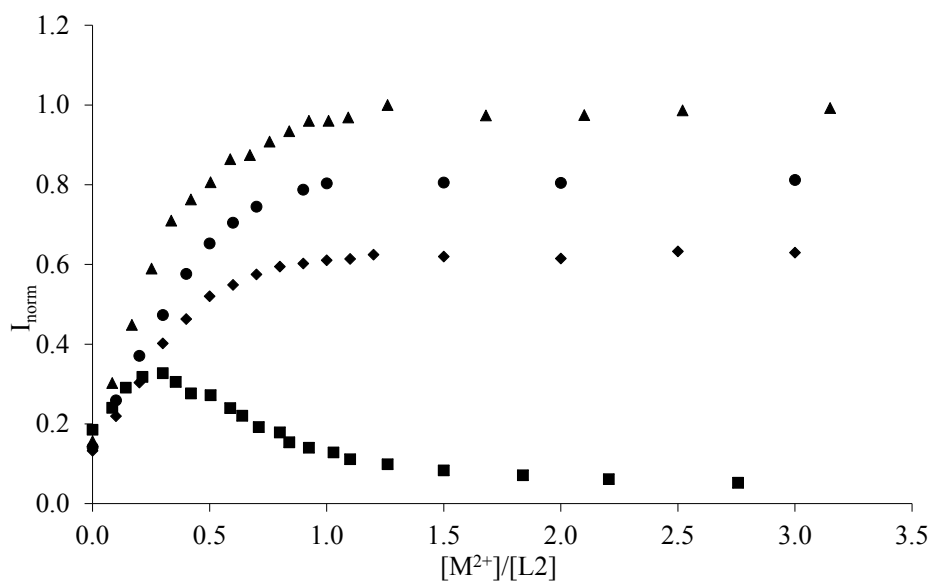


Figure S18. Normalized fluorescent intensity versus molar ratio plot for ligand L2 upon addition of increasing amounts of Cd^{2+} (▲), Zn^{2+} (●), Pb^{2+} (◆) and Cu^{2+} (■) ions ($[L2] = 1.99 \cdot 10^{-5}$ M, MeCN/ H_2O 4:1 v/v, 25 °C, $\lambda_{\text{ex}} = 323$, $\lambda_{\text{em}} = 358$ nm).

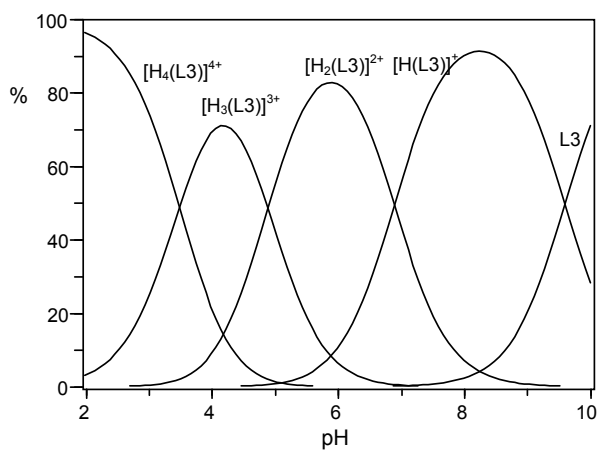
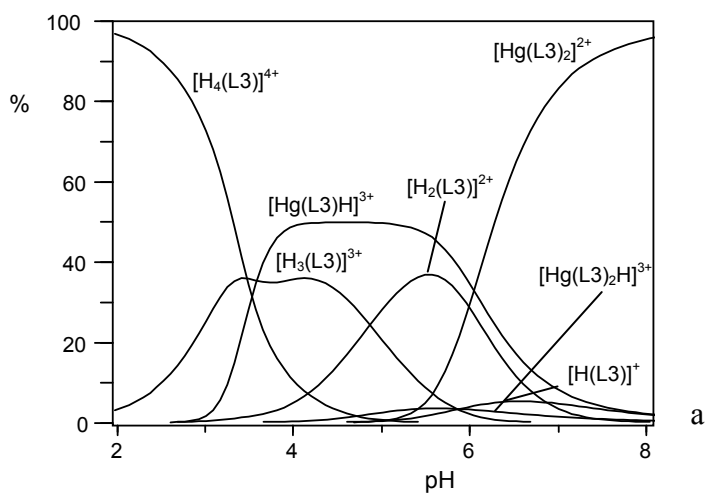
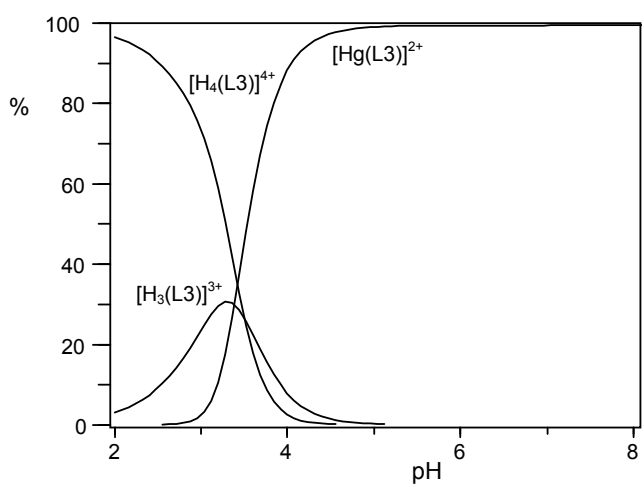


Figure S19. Distribution diagram of the protonated species of L3 ($[L3] = 0.001 \text{ M}$, $I = 0.1 \text{ M}$, $25 \text{ }^\circ\text{C}$)



a



b

Figure S20. Distribution diagrams of the species formed by Hg^{2+} with L3 in metal to ligand molar ratio 1:2 a) and 1:1 b) ($[\text{L3}] = 0.001 \text{ M}$, $I = 0.1 \text{ M}$, 25°C).

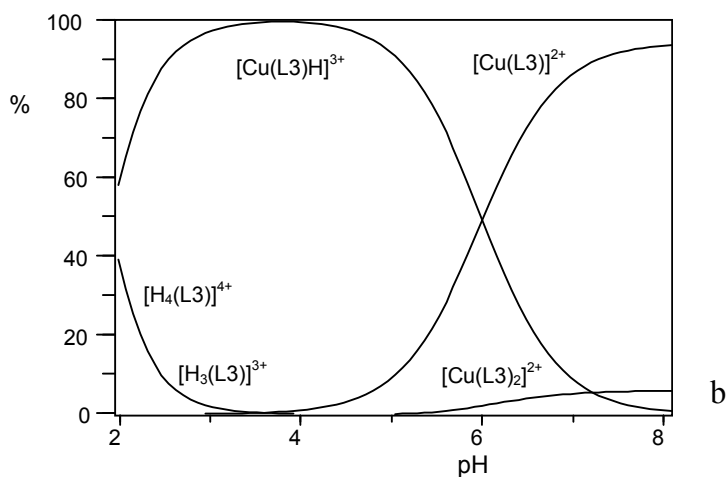
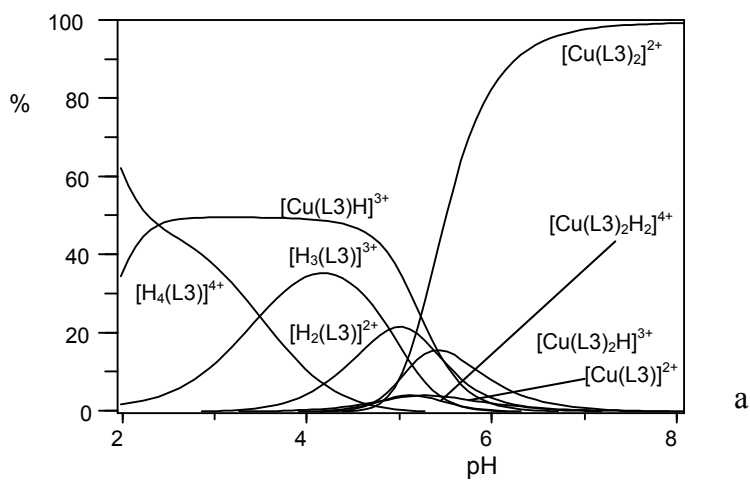


Figure S21. Distribution diagrams of the species formed by Cu^{2+} with L3 in metal to ligand molar ratio 1:2 a) and 1:1 b) ($[\text{L3}] = 0.001 \text{ M}$, $I = 0.1 \text{ M}$, 25°C).

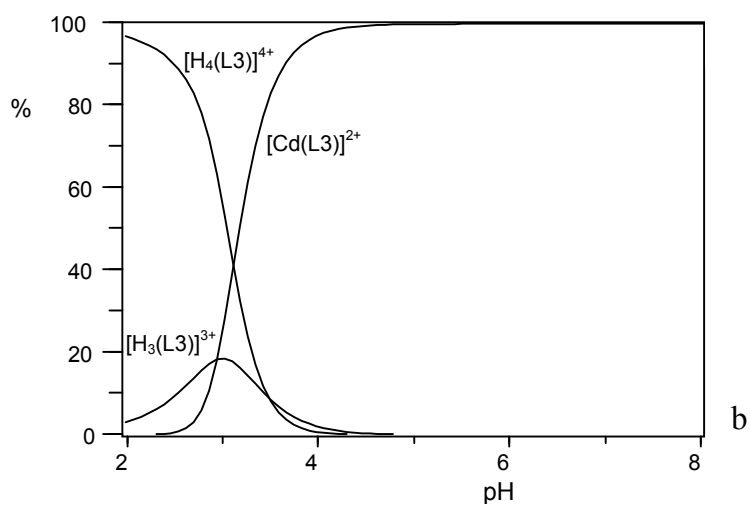
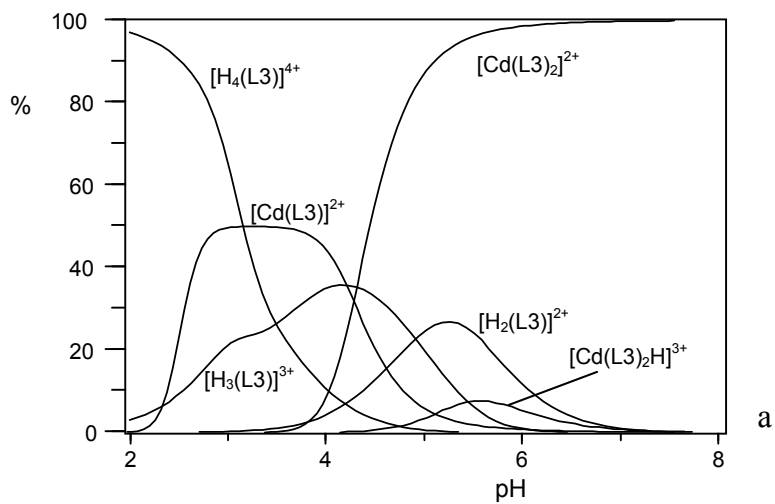


Figure S22. Distribution diagrams of the species formed by Cd^{2+} with L3 in metal to ligand molar ratio 1:2 a) and 1:1 b) ($[L_3] = 0.001$ M, $I = 0.1$ M, $25^\circ C$).

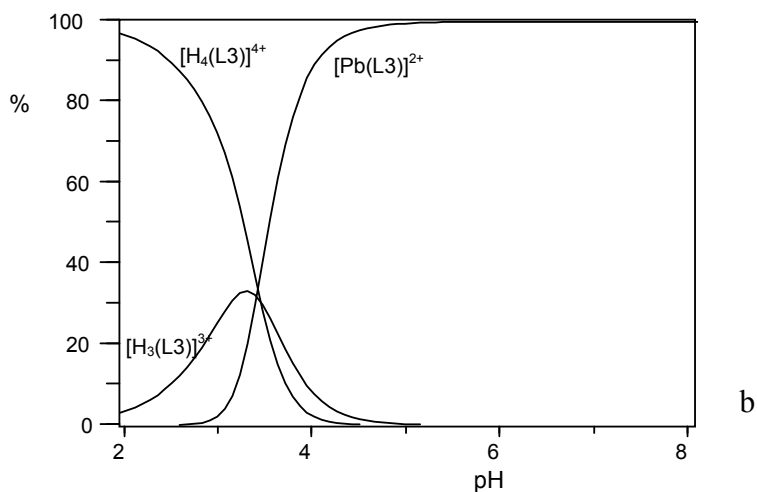
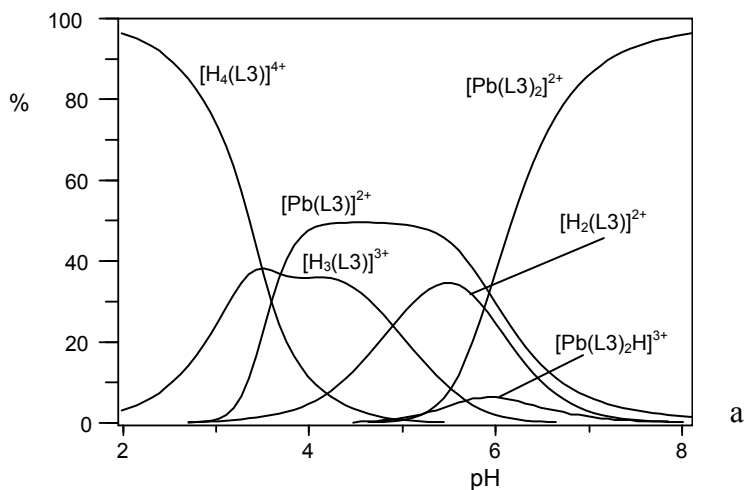
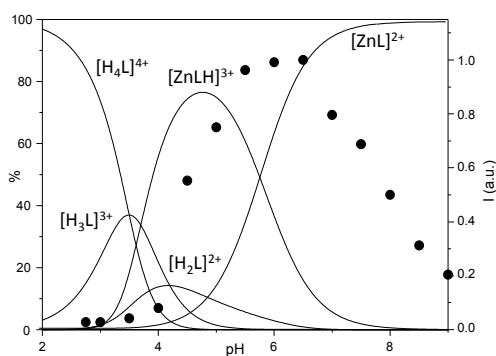
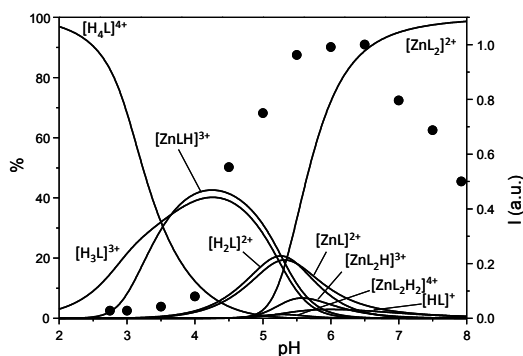


Figure S23. Distribution diagrams of the species formed by Pb^{2+} with L3 in metal to ligand molar ratio 1:2 a) and 1:1 b) ($[\text{L3}] = 0.001 \text{ M}$, $I = 0.1 \text{ M}$, 25°C).



a)



b)

Figure S24. Superimposition of the fluorescence emission intensity at 505 nm (right, y axis) with the distribution diagrams of the species formed by L3 in the presence of Zn^{2+} in a) 1:1 e b) 2:1 molar ratio (left, y axis, $[\text{L3}] = 1.95 \times 10^{-5} \text{ M}$). The decrease of the emission intensity above pH 7 can be ascribed to the formation of minor percentages of scarcely emissive hydroxo complexes.

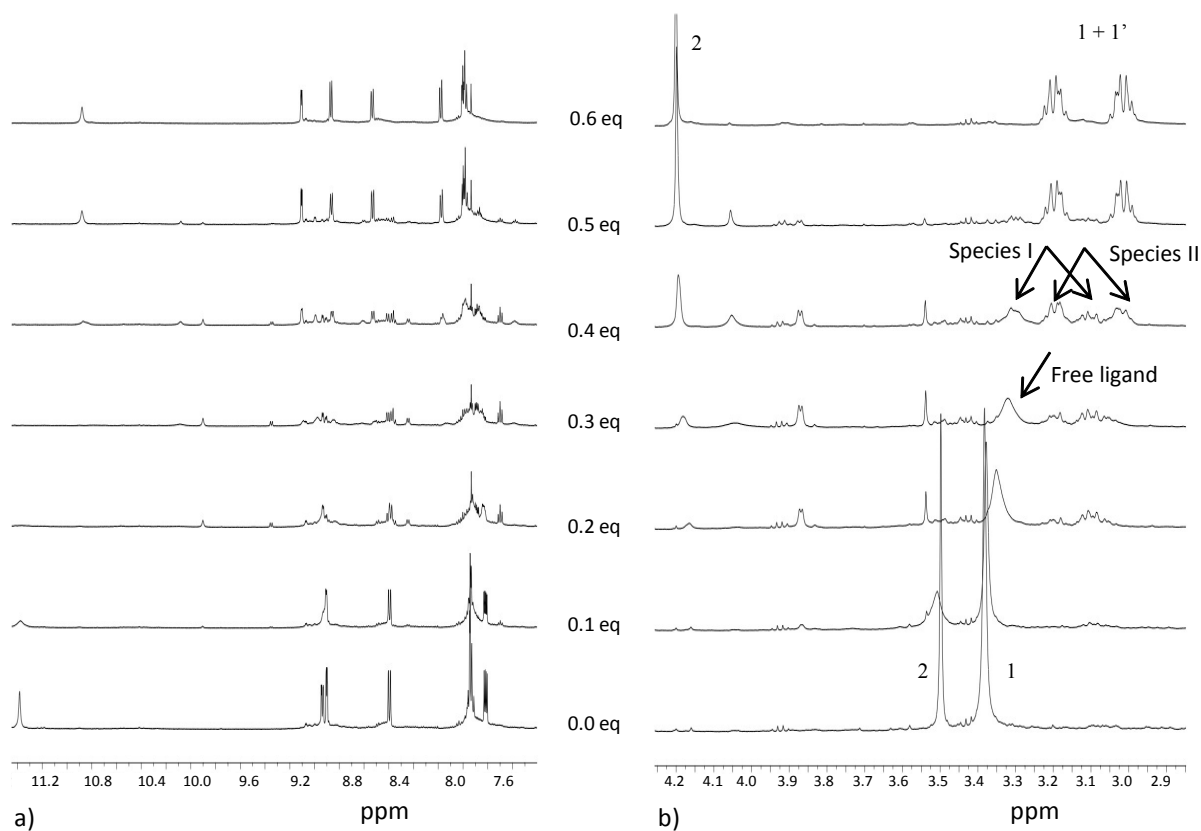


Figure S25. a) High and b) low frequency regions of the $^1\text{H-NMR}$ spectra of L3 in the presence of different amounts of Zn^{2+} . For the numbering scheme see Table 2.

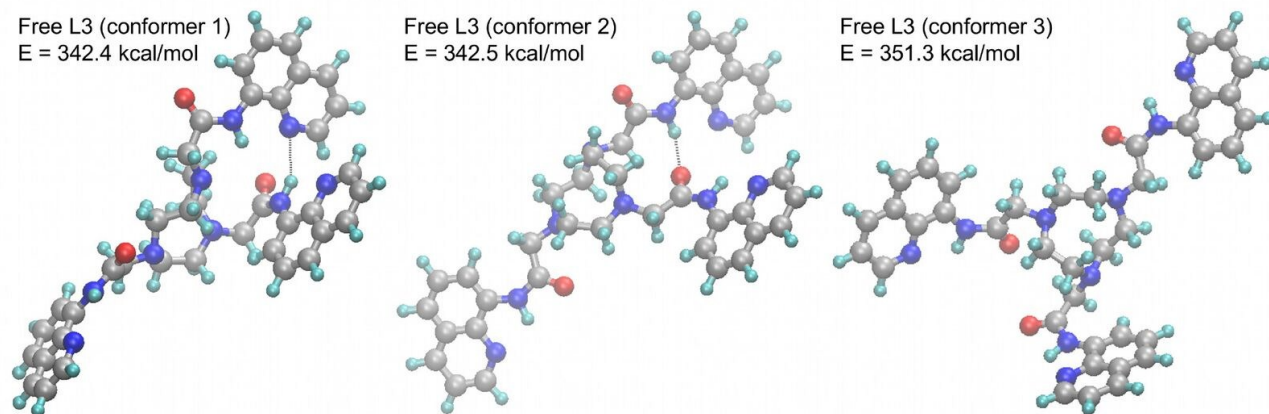
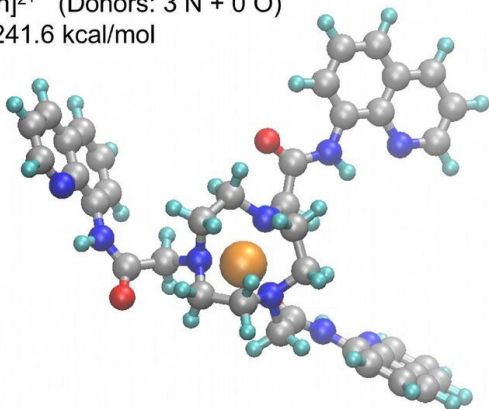
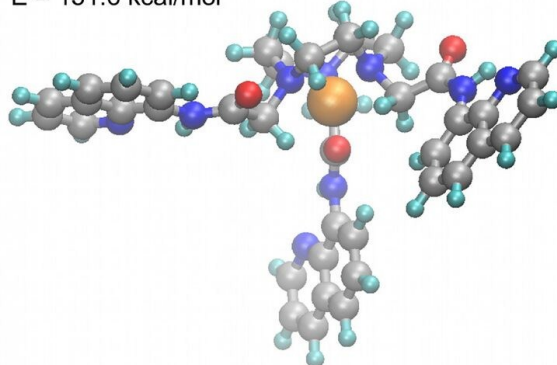


Figure S26. The three conformers with the lowest potential energy are shown (balls-and-sticks style) for L3 in the absence of any metal ion. The corresponding energy is reported in kcal/mol. Atoms are colour coded as: C (grey), H (cyan), N (blue) and O (red). Hydrogen-bonds are shown with dotted lines.

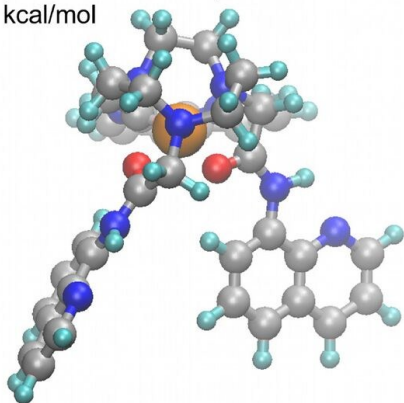
[L3Zn]²⁺ (Donors: 3 N + 0 O)
E = 241.6 kcal/mol



[L3Zn]²⁺ (Donors: 3 N + 1 O)
E = 151.6 kcal/mol



[L3Zn]²⁺ (Donors: 3 N + 2 O)
E = 107.6 kcal/mol



[L3Zn]²⁺ (Donors: 3 N + 3 O)
E = 288.0 kcal/mol

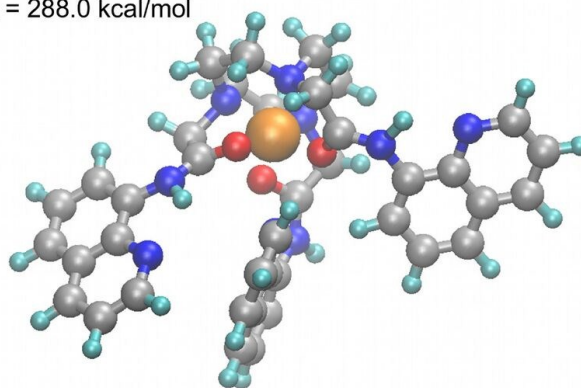


Figure S27. The lowest energy conformer is shown (balls-and-sticks style) for L3 in the presence of Zn²⁺. A different number of donors was considered in each case: 3 N (top-left), 3 N + 1 O (top-right), 3 N + 2 O (bottom-left) and 3 N + 3 O (bottom-right). The corresponding energy is reported in kcal/mol. Atoms are colour coded as: C (grey), H (cyan), N (blue) and O (red).

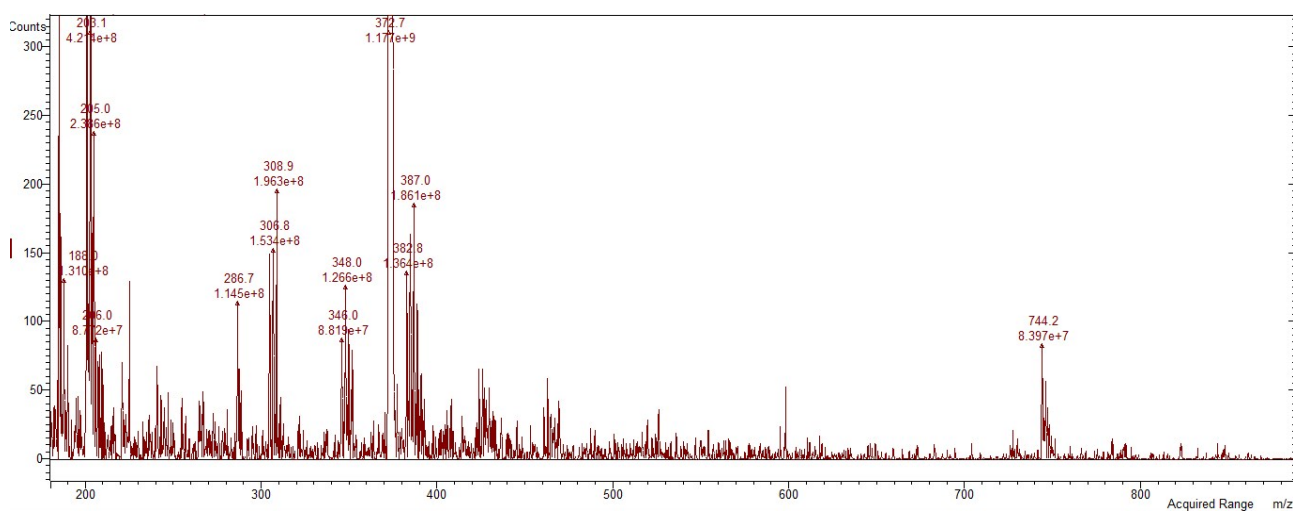


Figure S28. ESI-MS spectrum of a solution of L3 and Zn²⁺ at molar ratio Zn²⁺/L3 of 1.0 ([L3] = 0.001 M, MeCN/CHCl₃ 70:30 (v/v)).

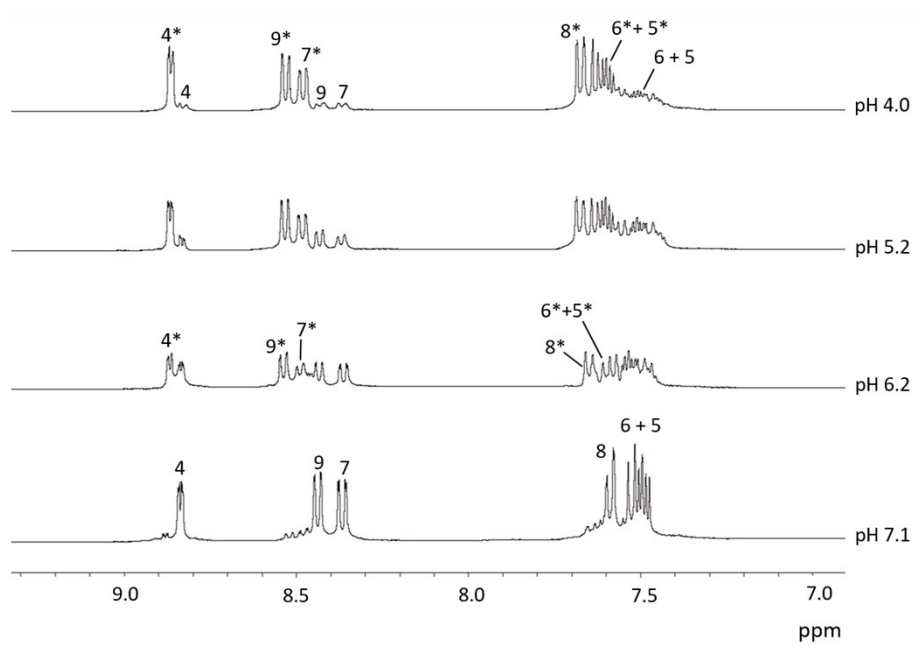
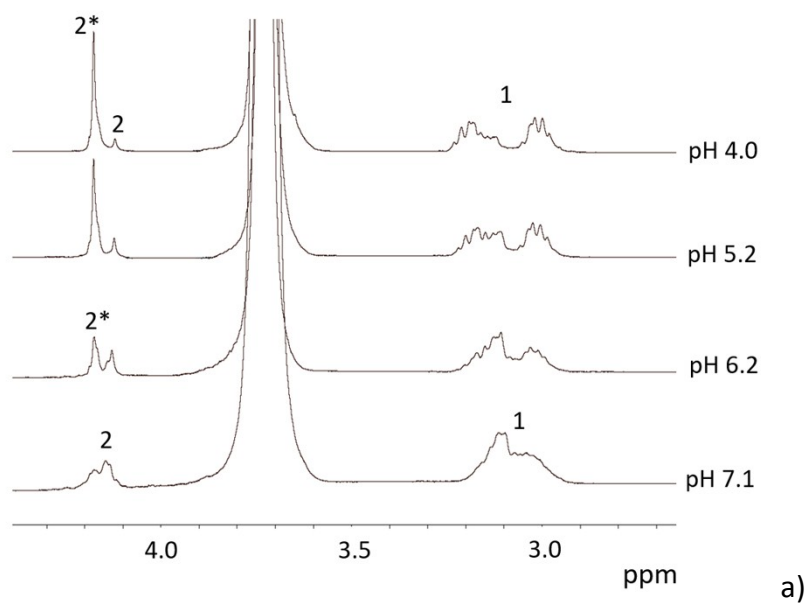
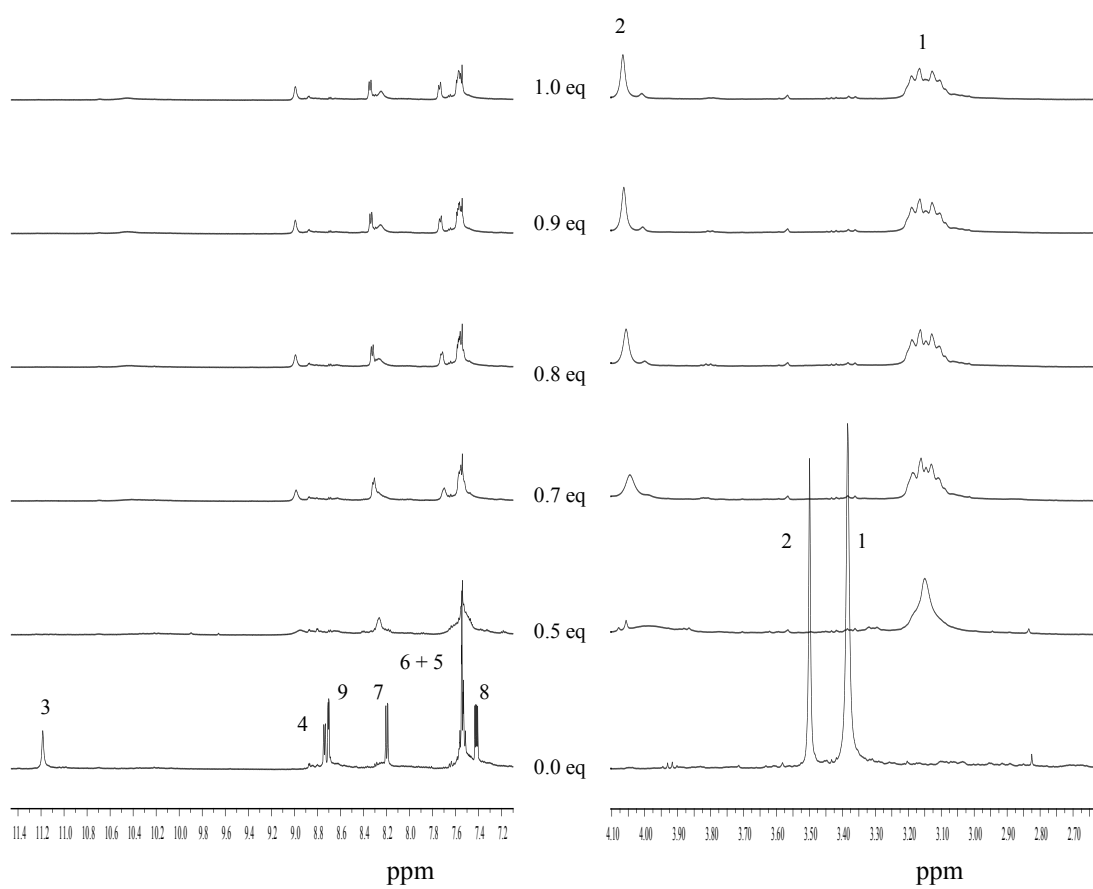


Figure S29. a) Low and b) high frequency regions of the ^1H -NMR spectra of L3 at different pH values in $\text{CD}_3\text{CN}:\text{D}_2\text{O}$ 1:1 v/v (signals labelled with an asterisk can be attributed to the protonated $[\text{ZnL3H}]^{3+}$ complex).



a)

b)

Figure S30. a) Low and b) high frequency regions of the $^1\text{H-NMR}$ spectra of L3 in the presence of different amounts of Hg^{2+} . For the numbering scheme see Table 2.

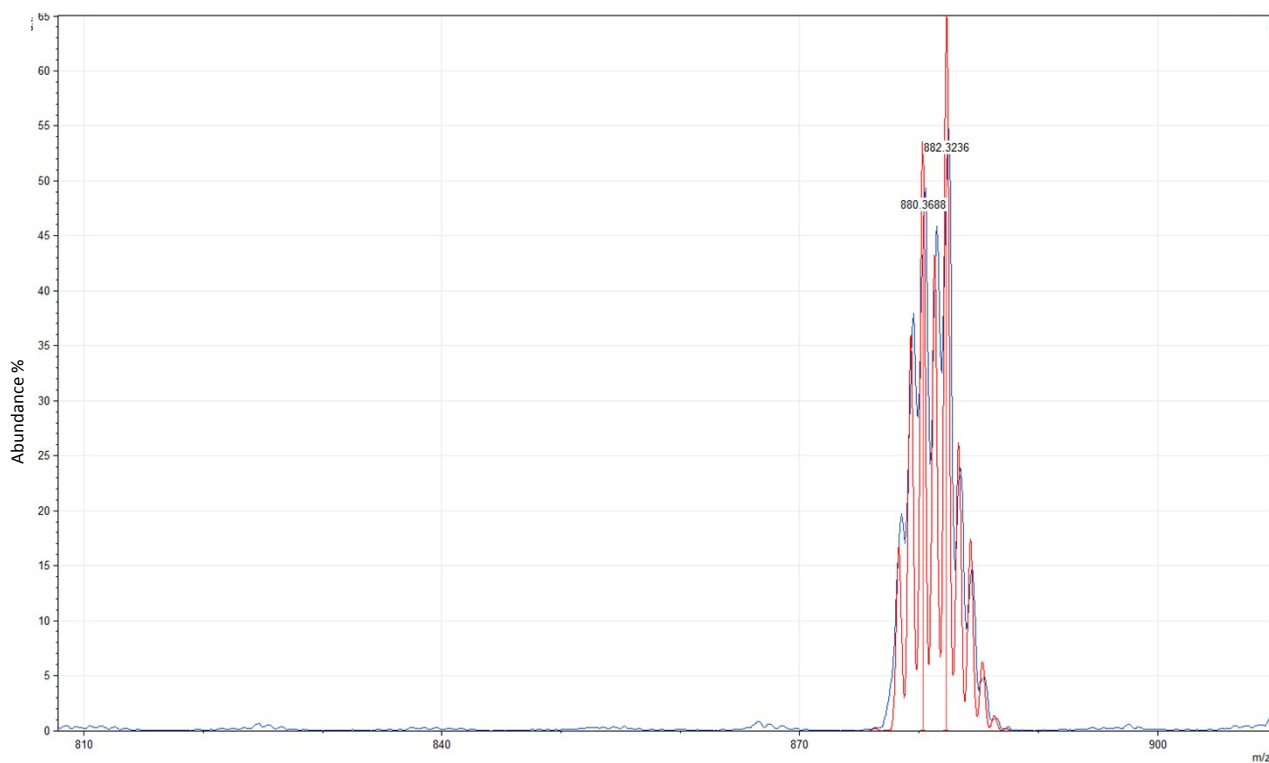


Figure S31. ESI-MS spectrum at molar ratio $\text{Hg}^{2+}/\text{L3}$ of 1.0 ($[\text{L3}] = 0.001 \text{ M}$, $\text{MeCN}/\text{CHCl}_3$ 70:30 (v/v)).

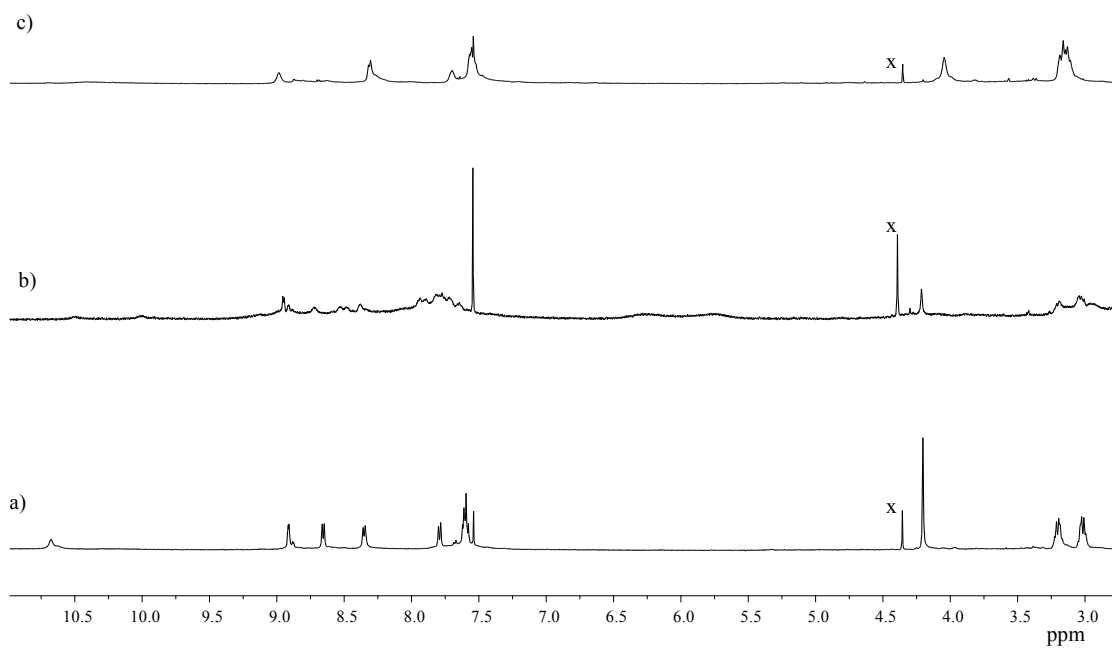


Figure S32. $^1\text{H-NMR}$ spectra of a) solution of L3 and Zn^{2+} at molar ratio $\text{Zn}^{2+}/\text{L3}$ of 1.0, b) solution of L3 and Zn^{2+} in 1:1 molar ratio and addition of 1 equiv. of Hg^{2+} and c) solution of L3 and Hg^{2+} at molar ratio $\text{Hg}^{2+}/\text{L3}$ of 1.0. (X = impurities).

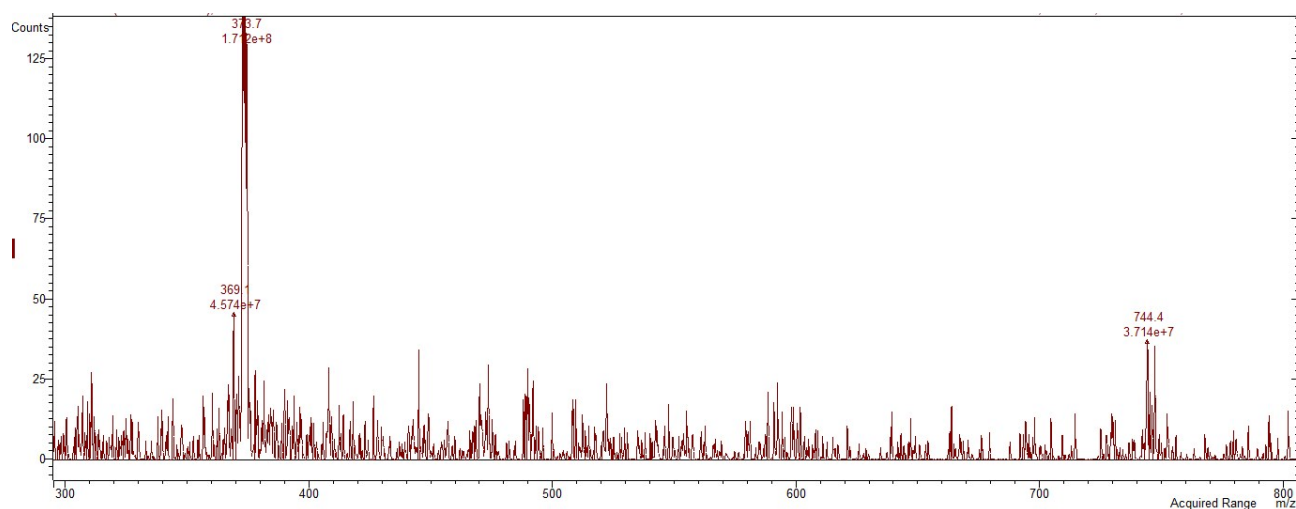


Figure S33. ESI-MS spectrum of a solution of L3 and Zn²⁺ in 1:1 molar ratio and addition of 1 equiv. of Hg²⁺ ([L3]= 0.001 M, MeCN/CHCl₃ 70:30 (v/v)).

Table S2. Summary of the basic crystallographic parameters for [ZnL1(Ac)](Ac) (1), [CuL1(Cl)](Cl)·H₂O (2) and [CuL3](NO₃) (3)

	1	2	3
Empirical formula	C ₃₅ H ₄₈ N ₉ O ₅ Zn, C ₂ H ₃ O ₂	C ₃₃ H ₄₆ Cl ₂ CuN ₉ O _{3.5}	C ₃₉ H ₃₈ CuN ₁₀ O ₆
Formula weight	799.24	759.23	806.34
Crystal system	triclinic	triclinic	orthorhombic
Space group	P-1	P-1	Pbca
a / Å	10.757(4)	10.2504(4)	16.8909(3)
b / Å	11.917(4)	12.2470(5)	10.8298(3)
c / Å	14.635(5)	15.0718(6)	39.2281(14)
α / °	88.72(3)	73.311(4)	90
β / °	85.72(3)	76.050(3)	90
γ / °	87.84(3)	88.129(3)	90
V / Å ³	1869.2(11)	1757.55(12)	7175.8(4)
T / K	295(2)	150(2)	120(2)
Z	2	2	8
Reflections collected	19785	16826	30968
Independent reflections	7511 [R _{int} = 0.023]	6826 [R _{int} = 0.027]	7048 [R _{int} = 0.0460]
Absorption correction	multi-scan	analytical	gaussian
Max. / min. transmission	1.000 / 0.764	0.924 / 0.662	0.786 / 0.896
Refinement method	Full-matrix least-squares on F ²	Full-matrix least-squares on F ²	Full-matrix least-squares on F ²
Data / restraints / parameters	7511 / 147 / 460	6826 / 0 / 442	7048 / 507 / 505
Goodness-of-fit on F ²	1.087	1.04	1.188
Final R indices [F ² > 2σ(F ²)]	R1 = 0.0375, wR2 = 0.1039	R1 = 0.0373, wR2 = 0.0943	R1 = 0.0981, wR2 = 0.2177
R indices (all data)	R1 = 0.0483, wR2 = 0.1065	R1 = 0.0463, wR2 = 0.101	R1 = 0.1031, wR2 = 0.2196

Table S3. Selected Bond Distances (Å) and Angles (°) for [ZnL1(Ac)](Ac) (1), [CuL1(Cl)](Cl)·H ₂ O (2) and [CuL3](NO ₃) (3).			
	1	2	3
M1-N1	2.0983(18)	2.2200(18)	1.928(5)
M1-N2			2.057(5)
M1-N3			2.081(5)
M1-N4	2.2318(19)	2.019(17)	2.044(5)
M1-N7	2.1048(19)	2.1159(18)	2.353(5)
M1-N41		2.1686(18)	
M1-O1	2.1473(17)		2.609(5)
M1-O3S	2.1179(18)		
M1-O4S	2.0889(18)		
M1-Cl1		2.2290(5)	
N1-M1-N2			82.7(2)
N1-M1-N3			165.7(2)
N1-M1-N4	82.24(7)	85.42(7)	81.8(2)
N1-M1-N7	85.23(7)	84.08(7)	100.6(2)
N1-M1-N41		106.37(7)	
N2-M1-N4			164.5(2)
N2-M1-N3			85.3(2)
N2-M1-N7			82.67(19)
N3-M1-N4			110.30(2)
N3-M1-N7			80.99(18)
N4-M1-N7	81.93(7)	85.12(7)	99.21(18)
N4-M1-N41		83.42(7)	
N7-M1-N41		163.76(7)	
N1-M1-O1	93.39(7)		106.5(2)
N1-M1-O3S	166.53(7)		
N1-M1-O4S	106.23(7)		
N2-M1-O1			96.2(2)
N3-M1-O1			71.6(2)
N4-M1-O1	169.60(6)		89.1(2)
N4-M1-O3S	95.19(7)		
N4-M1-O4S	98.92(7)		
N7-M1-O1	88.32(7)		152.5(2)
N7-M1-O3S	107.57(7)		
N7-M1-O4S	168.53(7)		
O1-M1-O3S	91.18(7)		
O1-M1-O4S	91.36(7)		
O3S-M1-O4S	60.97(7)		
N1-M1-Cl1		104.48(5)	
N4-M1-Cl1		167.98(7)	
N7-M1-Cl1		94.31(5)	
N41-M1-Cl1		94.99(5)	